



# Feasibility Study of R-Mode combining MF DGNSS, AIS, and eLoran Transmissions

Issue: 1.0  
Issue Status: Final Issue Date: 25/09/2014

Lead Authors: Dr. Gregory Johnson, Dr. Peter Swaszek

Prepared For: German Federal Waterways and Shipping Administration,  
Federal Waterways and Shipping Agency,  
Northern Region Office  
Jan-Hendrik Oltmann, Michael Hoppe

This report is part-financed by the EU Regional Development Fund.



## Executive Summary

High precision positioning in the maritime domain is now the norm since the introduction of Global Navigation Satellite Systems (GNSS). Unfortunately, it is well known that as low power, satellite-based systems, GNSS are vulnerable to interference (both naturally occurring and manmade); hence, the development of an alternative backup system is recommended. A variety of technological solutions to this backup requirement are possible; in the radio frequency (RF) domain we have the so-called “Signals of Opportunity” (SoOP) approach. This report considers several SoOP solutions to provide a Ranging Mode (R-Mode) Position Navigation and Timing (PNT) alternative to GNSS. This work is being done in support of the EU INTERREG IVb North Sea Region Programme project ACCSEAS (Accessibility for Shipping, Efficiency Advantages and Sustainability), which is a 3-year project supporting improved maritime access to the North Sea Region through minimising navigational risk.

Of interest to this study is the use of the Medium Frequency (MF) Differential GNSS (DGNSS) and the Automatic Identification System (AIS) broadcasts as SoOPs, both together and with existing eLoran signals:

- The Milestones 1 and 2 reports examined the R-Mode potential of the MF DGNSS signal; the recommended approach was to add CW signals to the broadcast and to develop the pseudorange from the carrier phase. Based on a narrowband sinusoidal signal, this approach requires resolution of the cycle ambiguity for use in ranging; options for accomplishing this were presented.
- The Milestones 3 and 4 reports examined the R-Mode potential of the AIS signal; the recommended approach was to estimate the pseudorange from the bit timing. The proposed solution is straightforward.
- eLoran is a long established positioning and timing signal and is currently broadcast from 5 stations around the North Sea area.

This report reviews each of these three signals, focusing assessments of effectiveness (through computation of best case positioning performance) on three areas in the North Sea Region as shown in **Figure 1**. Region I covers much of the North Sea to examine effectiveness over longer distances, region II focuses on a coastline area with many MF DGNSS and AIS transmitters, and region III zooms in on two inland waterways, the Kiel Canal and the Elbe River. As part of the review of each signal type, modifications that would be required to the transmitters for their use in R-Mode, if necessary, are reviewed. In short, it is noted that MF DGNSS R-Mode would require a new transmitter (with precise time synchronization), AIS R-Mode would require precise synchronization of existing transmitters and the use of additional transmissions, and eLoran transmitters would require no changes.

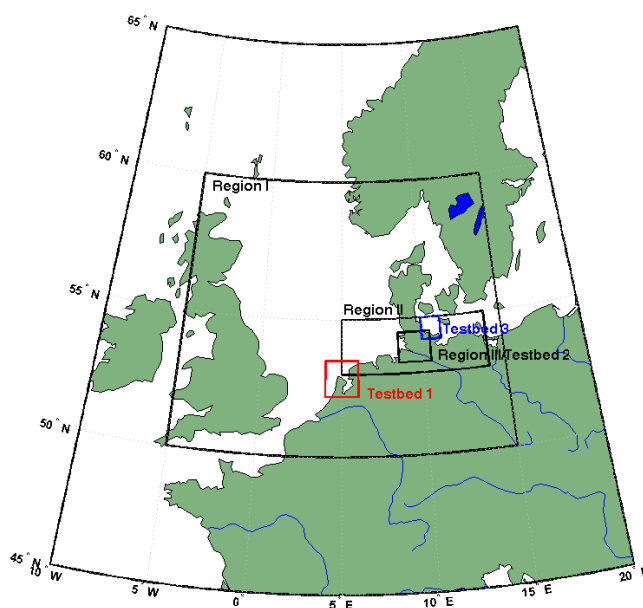
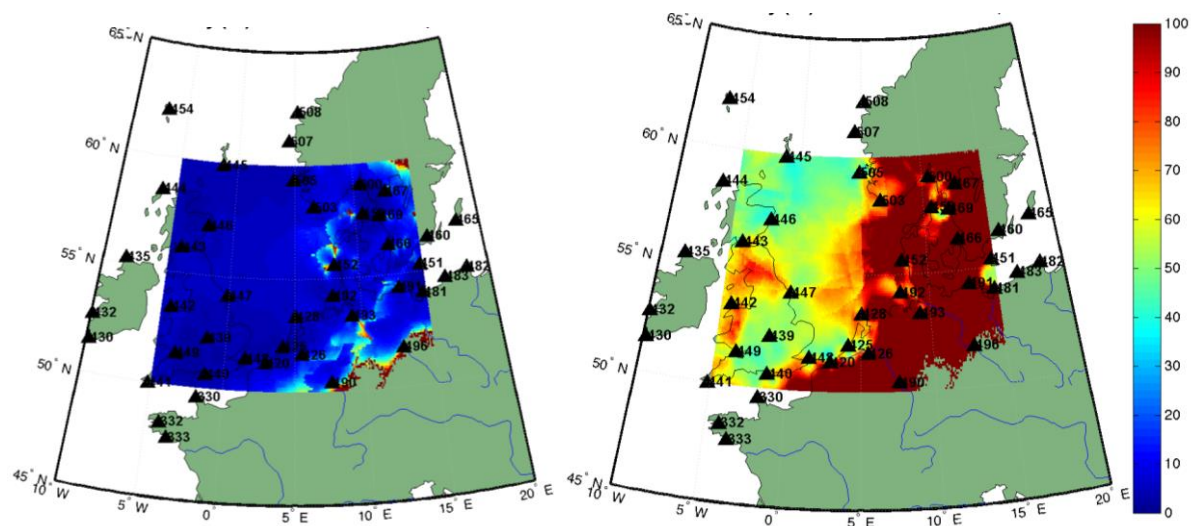


Figure 1: Regions of interest near the North Sea



**Figure 2: MF DGNSS R-Mode day (left) and night (right) predicted positioning accuracy (m) using a 0-100m scale.**

The performance assessments for each of the three signal types are the calculated lower bounds to positioning accuracy, but are based upon assumptions that are very conservative. Being trilateration solutions for position of signals from terrestrial transmitters, the resulting performance is a function of the received signal power (estimated using modelling software), the observation time of the receiver (nominally assumed to be 5 seconds), and the geometry of the known transmitter locations. For each signal type the sources of error not included in the performance assessment are described. Examples of such sources include the unknown offsets in the synchronization of the employed transmitters (this is relevant to all three signals) and propagation delays that would increase the observed range estimates (this is known to impact both MF and eLoran signals since they propagate as ground waves). To summarize results:

- **MF DGNSS R-Mode is a backup to GNSS that can meet the resilient PNT requirements of e-Navigation.** The MF DGNSS signals are at sufficient power levels and the transmitters are well enough distributed geographically so as to provide good coverage over the North Sea region and good performance during the day; at night, while the coverage is still good, sky wave interference greatly reduces range accuracy (see Figure 2). Further, ambiguity resolution is a non-trivial problem for these CW signals. Propagation delays of the ground wave might also need to be estimated and mapped.
- **AIS R-Mode is a backup to GNSS that can meet the resilient PNT requirements of e-Navigation.** The AIS signals are also at sufficient power levels and are well distributed geographically so as to provide good performance (see Figure 3) for users within line-of-sight reception (the coverage area is a direct function of the transmit antenna height). The primary limiting factor of AIS ranging is the short propagation distance of the signal, which limits the coverage area provided by such a system since a user must receive signals from at least three different AIS base stations to solve for latitude and longitude.
- The eLoran signals provide good coverage over the North Sea region. To achieve high accuracy, the propagation delays of the ground wave would need to be estimated and mapped. The primary limiting factor of eLoran is the continued uncertainty regarding the future of eLoran and the limited number of transmitters.

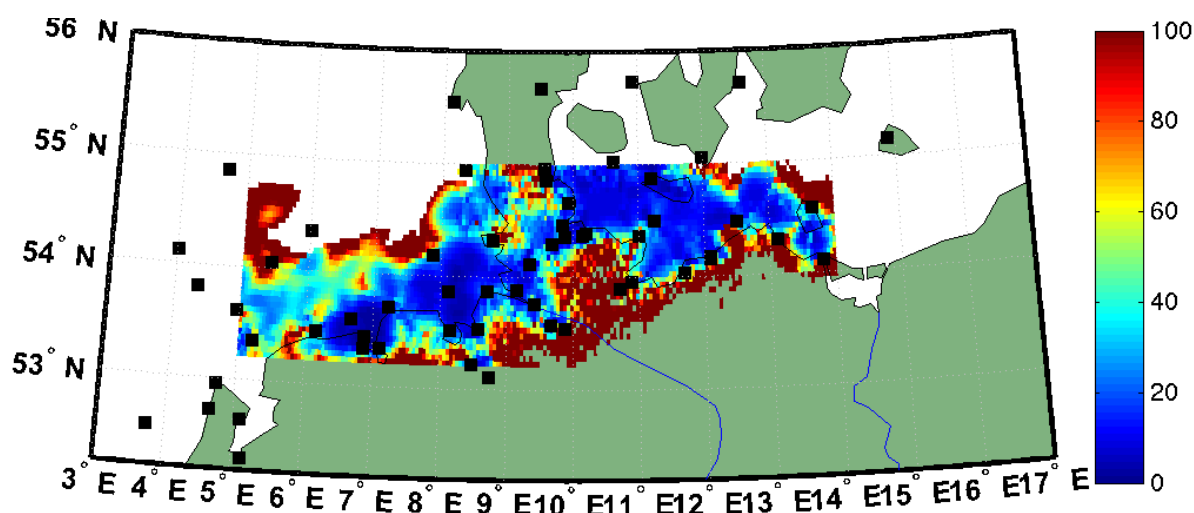


Figure 3: AIS R-Mode predicted positioning accuracy (m) using a 0-100m scale.

Of primary interest in this report is combining the R-Mode signals for a better position solution. Toward that end, this report describes the architecture of an “all-in-view” receiver that could combine signals from two or more of these sources. The potential performance of this all-in-view receiver is then computed for the three regions of interest with various combinations of the three signals to demonstrate potential synergies. Focusing on region II (where computations are available for all 3 signals), Table 1 shows the relative levels of performance for the various combinations. As expected, the best performance can be achieved using ALL signals. Performance at night is slightly worse than during the day due to the reduced MF DGNSS performance at night. A single eLoran station can provide a large improvement at night over a large coverage area. Sylt alone for example, can cover the North and Baltic Seas sufficiently as an R-Mode signal to supplement AIS or MF DGNSS R-Mode; it is a very efficient augmentation to AIS R-Mode. Also, even a single strategically positioned eLoran station can provide cost-efficient time transfer for all R-Mode MF and AIS shore stations in the area; precise timing of transmissions is one of the fundamental prerequisites for any R-Mode at MF and/or AIS shore stations in the region.

Table 1: Pairwise synergy of the signal choices.

1 = 0-10m, 2 = 0-20m, 3 = 0-50m, and 4 = 0-100m position accuracy over most of the area

System	Performance
MF DGNSS(day)-AIS-eLoran(1)	1
MF DGNSS(day)-AIS	1
MF DGNSS(day)-eLoran(1)	2
MF DGNSS(night)-AIS-eLoran(1)	2
AIS-eLoran(1)	2
MF DGNSS(day)	2
MF DGNSS(night)-AIS	3
AIS	3
eLoran (5)	3
MF DGNSS(night)-eLoran(1)	4
MF DGNSS(night)	4
eLoran (1)	n/a

In summary, depending upon availability, 1 or 2 eLoran signals can be combined with AIS and MF DGNSS to offer improved performance. In general performance results are strongly position dependent – in many areas one system (signal type) dominates performance. Also, as expected, more signals results in increased performance (or at least no worse). **To achieve widespread resilient PNT, the best solution is to use all signals available in a true all-in-view receiver.**

It is also important to note that the need for a backup PNT is not uniform. The performance of a backup PNT system is most critical in the areas with the highest density of shipping traffic. Figure 4 shows the predicted R-Mode performance for region II overlaid on top of the ACCSEAS shipping density plot to illustrate this alignment. It is likely that this alignment of R-Mode performance with the high density shipping lanes will be true in other parts of the world as well, since those are the areas with the largest numbers of AIS (and MF DGNSS) stations.

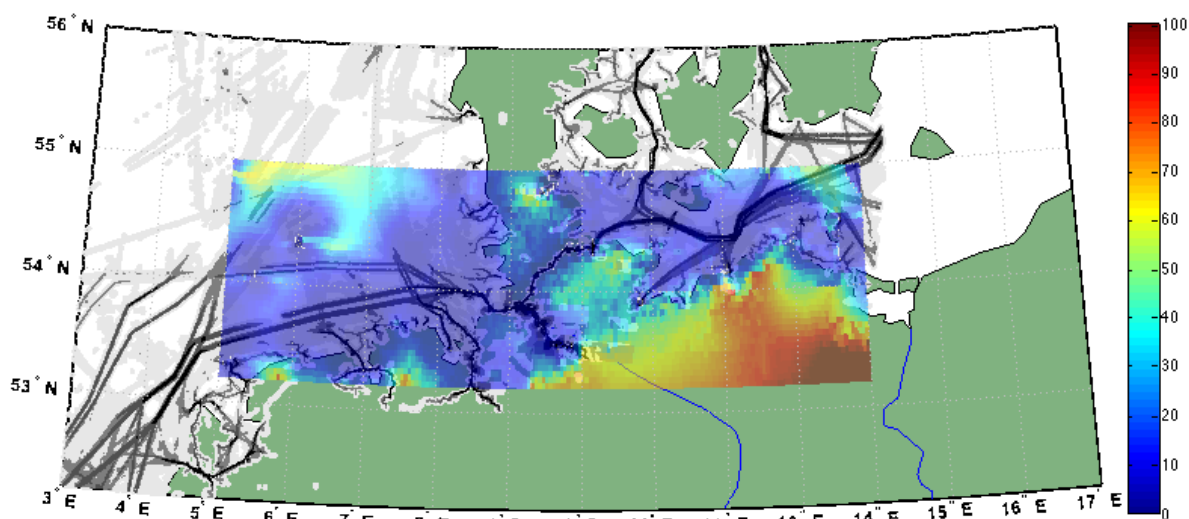


**Figure 4: R-Mode performance overlaid on top of shipping density plot.**  
**Predicted R-Mode performance shaded using 0-100m accuracy scale. Shipping density shaded so that darker is higher density traffic.**

Finally, looking toward future experimental testing of an R-Mode system, three alternatives for a potential R-Mode test bed are proposed: one on the Dutch coast near Amsterdam (test bed 1 in red in Figure 1), one focused on German transmitters covering the Kiel Canal and Elbe River (test bed 2/region III in Figure 1), and one on the western Baltic combining transmitters in Germany and Denmark (test bed 3 in Figure 1). Establishing a test bed would allow for testing to assess the performance of a real-world receiver (versus the predicted lower bounds on performance) and also to investigate the impact of time synchronization and propagation effects.



## Table of Contents

<b>1</b>	<b>Introduction .....</b>	<b>10</b>
1.1	Background .....	10
1.2	Regional Context .....	10
<b>2</b>	<b>Review of the Potential Signals.....</b>	<b>13</b>
2.1	The MF DGNSS Broadcast.....	13
2.1.1	Estimating the TOA .....	13
2.1.2	Geometry and Signal Strength.....	15
2.1.3	Positioning Accuracy .....	15
2.1.4	R-Mode Receiver.....	17
2.2	The AIS Broadcast.....	18
2.2.1	Estimating the TOA .....	18
2.2.2	Geometry and Signal Strength.....	19
2.2.3	Positioning Accuracy .....	20
2.2.4	R-Mode Receiver.....	21
2.3	eLoran .....	22
2.3.1	Estimating the TOA .....	22
2.3.2	Geometry and Signal Strength.....	24
2.3.3	Positioning Accuracy .....	26
2.3.4	eLoran Receiver .....	28
<b>3</b>	<b>Combining Ranging Signals.....</b>	<b>29</b>
3.1	The Truly “All-in-View” Receiver .....	29
3.2	MF DGNSS and eLoran.....	31
3.3	MF DGNSS and AIS .....	33
3.4	MF DGNSS, AIS, and eLoran .....	36
3.4.1	Region II .....	36
3.4.2	Region III .....	37
3.5	Test Bed Design .....	41
3.5.1	Test Bed Option 1 – German-Dutch.....	41
3.5.2	Test Bed Option 2 – German.....	42
3.5.3	Test Bed Option 3 – German-Danish.....	43
<b>4</b>	<b>Conclusions .....</b>	<b>44</b>
<b>5</b>	<b>References.....</b>	<b>48</b>

## Table of Figures

Figure 1: Regions of interest near the North Sea .....	2
Figure 2: MF DGNSS R-Mode day (left) and night (right) predicted positioning accuracy (m) using a 0-100m scale.....	3
Figure 3: AIS R-Mode predicted positioning accuracy (m) using a 0-100m scale. ....	4
Figure 4: R-Mode performance overlaid on top of shipping density plot. Predicted R-Mode performance shaded using 0-100m accuracy scale. Shipping density shaded so that darker is higher density traffic. ....	5
Figure 5: Ship traffic density in the NSR reprinted from [1]. The labels show the total number of ships passing each line from both directions during 2012. The red colour gradient shows the relative density of shipping in the NSR. The empty area in the middle of the North Sea is an area without AIS coverage (it does not mean that there is no traffic). ....	11
Figure 6: The overarching e-Navigation architecture from [2]. ....	12
Figure 7: IMO overarching e-Navigation Architecture represented as “7 Pillars”, reprinted from [1]. ....	12
Figure 8: The Cramer-Rao lower bound on performance of estimating the time of arrival from the phase of the MF ranging signal as a function of signal to noise ratio. ....	14
Figure 9: HDOP from the MF DGNSS sites (shown as triangles) for region I. ....	15
Figure 10: Lower bound to positioning accuracy of MF DGNSS R-Mode (in meters) – day. ....	16
Figure 11: Lower bound to positioning accuracy of MF DGNSS R-Mode (in meters) – night. ....	17
Figure 12: MF DGNSS R-Mode receiver. ....	18
Figure 13: The Cramer-Rao lower bound on performance of estimating the time of arrival from the AIS bit transition as a function of the received signal level in dBm. ....	19
Figure 14: HDOP for the AIS base stations (shown as squares) in region II. ....	20
Figure 15: Lower bound to positioning accuracy of AIS R-Mode (in meters) in region II (AIS stations shown as black squares). ....	21
Figure 16: AIS R-Mode receiver. ....	21
Figure 17: Typical performance of estimating the time of arrival from the eLoran signal as a function of the received signal strength in dB $\mu$ V (reprinted from [7]). ....	22
Figure 18: eLoran transmitter locations (shown as red dots) relevant to the regions of interest (I, II, and III) and test beds (1, 2, and 3). ....	24
Figure 19: HDOP for the five eLoran stations in region I); Loran towers marked with black circles (Ejde is located to the NW just off the plot). ....	25
Figure 20: Predicted signal strength for a typical eLoran site, Sylt (in dB $\mu$ V); Sylt is indicated by the black circle. ....	26

Figure 21: Lower bound to positioning accuracy of eLoran (in meters); Loran towers marked with black circles (Ejde is located to the NW just off the plot).....	27
Figure 22: Lower bound to positioning accuracy of eLoran (in meters) with just three stations; Loran towers marked with black circles. ....	28
Figure 23: eLoran receiver. ....	29
Figure 24: MF+AIS+eLoran “All-in-View” R-Mode receiver.....	30
Figure 25: Lower bound to positioning accuracy of combined MF DGNSS R-Mode and eLoran on region I – night.....	31
Figure 26: Lower bound to positioning accuracy of combined MF DGNSS and eLoran (Sylt only) on region I – night.....	32
Figure 27: Lower bound to positioning accuracy of combined MF DGNSS and eLoran (Sylt and Anthorn) on region I - night.....	32
Figure 28: Lower bound to positioning accuracy of combined MF DGNSS and eLoran (Sylt and Anthorn) on region I – night with Ekofisk added.....	33
Figure 29: Lower bound to positioning accuracy of MF DGNSS R-Mode on region II – day. ....	34
Figure 30: Lower bound to positioning accuracy of MF DGNSS R-Mode on region II – night. ....	34
Figure 31: Lower bound to positioning accuracy of combined MF DGNSS and AIS R-Mode on region II– day. MF beacon locations are triangles, AIS stations are squares. ....	35
Figure 32: Lower bound to positioning accuracy of combined MF DGNSS and AIS R-Mode on region II– night. MF DGNSS beacon locations are triangles, AIS stations are squares. ....	35
Figure 33: Lower bound to positioning accuracy of combined MF DGNSS-AIS-eLoran (Sylt only) on region II- night.....	36
Figure 34: Lower bound to positioning accuracy of combined MF DGNSS-AIS-eLoran (Sylt and Anthorn) on region II- night.....	36
Figure 35: Lower bound to positioning accuracy of AIS R-Mode on region III (in meters). AIS sites are squares. ....	37
Figure 36: Combined AIS and MF GNSS R-Mode performance on region III – day; AIS sites are squares, MF DGNSS sites are triangles.....	38
Figure 37: Combined AIS and MF DGNSS R-Mode performance on region III – night. AIS sites are squares, MF DGNSS sites are triangles.....	38
Figure 38: Lower bound to positioning accuracy of combined AIS and eLoran (Sylt only) on region III. AIS sites are squares, Sylt is a circle. ....	39
Figure 39: Combined MF DGNSS, AIS, and eLoran (Sylt only) on region III – night. AIS sites are squares, MF DGNSS sites are triangles, Sylt is a circle. ....	40
Figure 40: Combined MF DGNSS , AIS, and eLoran (Sylt and Anthorn) on region III – night. AIS sites are squares, MF DGNS sites are triangles, Loran are circles.....	40
Figure 41: IJmuiden test transmitter with 100km range ring; AIS sites are red dots, MF DGNSS test transmitter is black dot. ....	41



Figure 42: Option 1 for a test bed area near Ijmuiden. Predicted coverage accuracy using AIS, MF DGNSS, and eLoran (Sylt only) R-Mode during the day (night coverage is similar).....	42
Figure 43: Option 2 for a test bed area near the Kiel Canal and Elbe River. Predicted coverage accuracy using AIS, MF DGNSS, and eLoran (Sylt only) R-Mode during the day (night coverage is similar). ....	43
Figure 44: Option 3 for a joint German-Dutch test bed area. Predicted coverage accuracy using AIS (squares), MF DGNSS (Groß Mohrdorf to East, not visible), and eLoran (Sylt only, not visible on map) R-Mode during the night. ....	44
Figure 45: R-Mode performance overlaid on top of shipping density plot. Predicted R-Mode performance shaded using 0-100m accuracy scale. Shipping density shaded so that darker is higher density traffic. ....	47
Figure 45: R-Mode performance overlaid on top of shipping density plot. Predicted R-Mode performance shaded using 4-point scale defined for Table 2. Shipping density shaded so that darker is higher density traffic.....	47

## List of Tables

Table 1: Pairwise synergy of the signal choices. ....	4
Table 2: Pairwise synergy of the signal choices. ....	46

## 1 Introduction

### 1.1 Background

High precision positioning in the maritime domain is now the norm since the introduction of Global Navigation Satellite Systems (GNSS). Unfortunately, it is well known that as low power, satellite-based systems, GNSS are vulnerable to interference (both naturally occurring and manmade); hence, the development of an alternative backup system is recommended.

A variety of technological solutions to this backup requirement are possible; in the radio frequency (RF) domain we have the so-called “Signals of Opportunity” (SoOP) approach. This term refers to the opportunistic use of RF signals, typically communications signals, which exist in the geographical area of the receiver. While these signals are not primarily intended for positioning, a SoOP navigation receiver attempts to exploit them as such. Specifically, if each SoOP can provide a (pseudo-)range to the receiver from a known location, a trilateration position solution is possible. Even if a complete position solution is impossible from the SoOP (perhaps due to too few signals being present), the resulting pseudorange information could be combined with measurements from existing positioning systems in a position solution (e.g. combined perhaps with GNSS measurements limited by urban canyons).

Of interest to this study is the integrated use of the Medium Frequency Differential GNSS (MF DGNSS) broadcasts and Very High Frequency (VHF) Automatic Identification System (AIS) broadcasts, both together and as combined with eLoran. This report considers the performance of several integrated solutions to provide a Ranging Mode (R-Mode) Position Navigation and Timing (PNT) alternative to GNSS.

### 1.2 Regional Context

This work is being done in support of the EU INTERREG IVb North Sea Region Programme project ACCSEAS (Accessibility for Shipping, Efficiency Advantages and Sustainability), which is a 3-year project supporting improved maritime access to the North Sea Region through minimising navigational risk. The goals of the ACCSEAS project are to<sup>1</sup>:

- identify key areas of shipping congestion and limitation of access to ports;
- define solutions by prototyping and demonstrating success in an e-Navigation test-bed at the North Sea regional level.

The North Sea Region (NSR) as defined by ACCSEAS [1] includes the eastern part of the United Kingdom, Belgium, the Netherlands, the northern part of Germany, Denmark, the southern part of Norway, and the western part of Sweden as well as the Skagerrak and Kattegat, the Sounds and the south-western part of the Baltic Sea. The three largest and busiest ports in the NSR are Rotterdam, Antwerp, and Hamburg. This area is shown in Figure 5 with ship traffic densities in red. Based on the traffic and risk analysis done using the International Association of Marine Aids to Navigation and Lighthouse Authorities (IALA) IWRAP model, about 70% of the predicted collisions take place north of Germany and the Netherlands, making this a key area for testing and implementation of R-Mode.

---

<sup>1</sup> From <http://www.accseas.eu/about-accseas>.

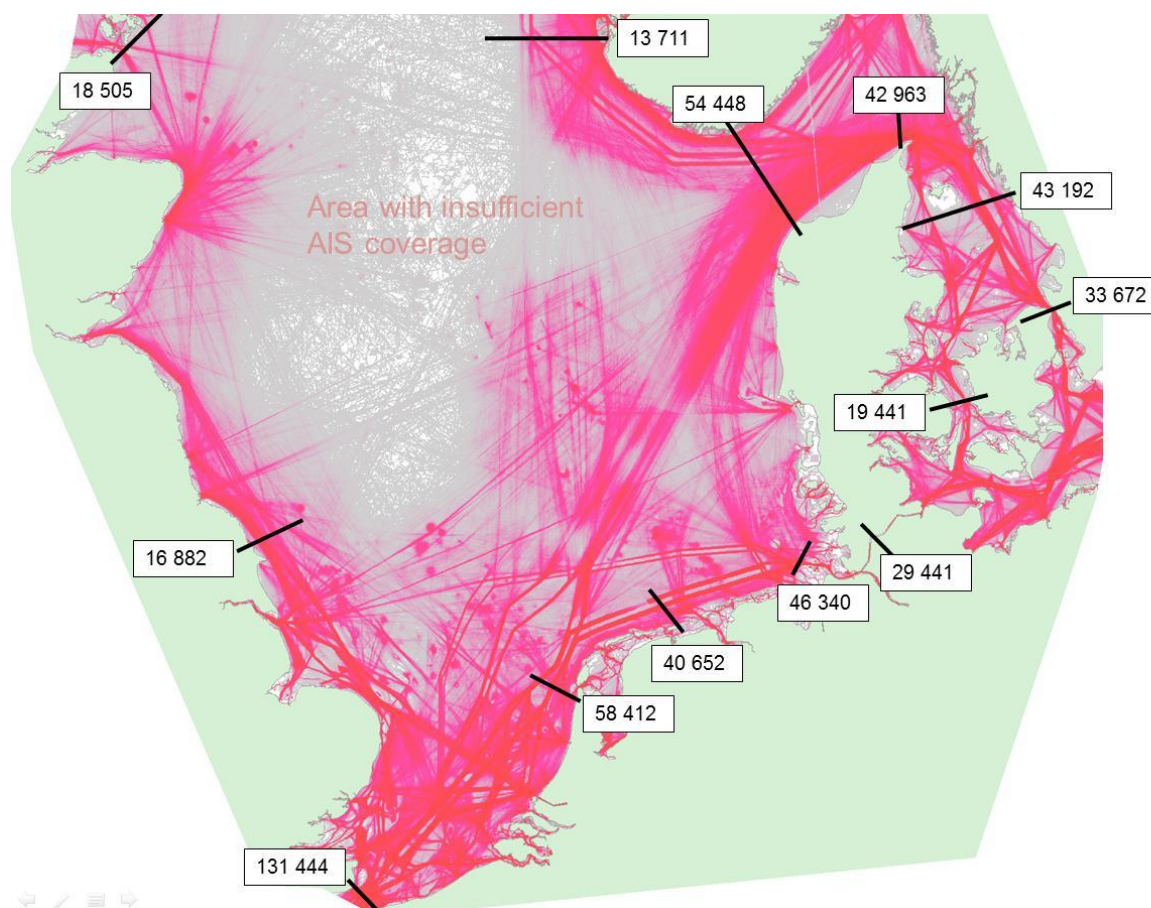


**Figure 5: Ship traffic density in the NSR reprinted from [1]. The labels show the total number of ships passing each line from both directions during 2012. The red colour gradient shows the relative density of shipping in the NSR. The empty area in the middle of the North Sea is an area without AIS coverage (it does not mean that there is no traffic).**

The recently released “Baselines and Priorities Report” [1] contains an analysis of the traffic in the region, both current and projected. The planned enormous expansion of wind farms will reduce the navigable space and could impact key shipping lanes, raising safety and efficiency concerns. The report also traces user needs to system requirements using a system engineering approach. One of the low level user requirements identified was the need for resilient PNT.

The ACCSEAS project activities are aligned with the IMO e-Navigation concept as shown in Figure 6. This can also be visualized as the so-called “7 Pillars of e-Navigation” as shown in Figure 7. The pillar of interest to this report is the Resilient PNT pillar which is defined as “Highly reliable and robust determination of Position, Navigation data and Time (PNT) at the shipboard and shore-based electronic systems with the World Wide Radio Navigation System (WWRNS) of IMO at the core” [1]. The ACCSEAS potential solution that maps to this pillar is the Multi-Source Positioning Service (MSPS). “The resilient PNT technical services - e.g. Ranging Mode (R-Mode) – that are based on backup technologies independent of GNSS could be central to the e-Navigation and test-bed architectures to meet the user need for resilient PNT. These technical services could support a MSPS operational service that would provide, monitor and distribute resilient PNT information to a broad range of e-Navigation operational services” [1].

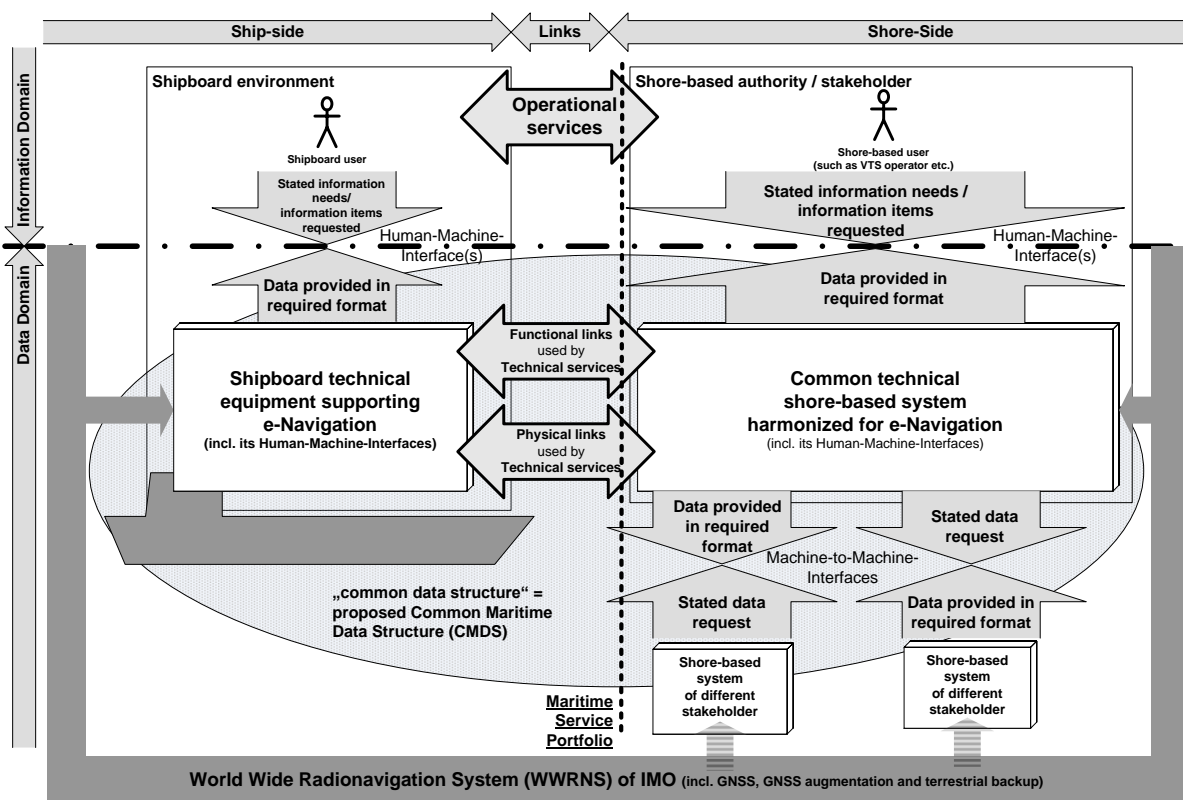


Figure 6: The overarching e-Navigation architecture from [2].

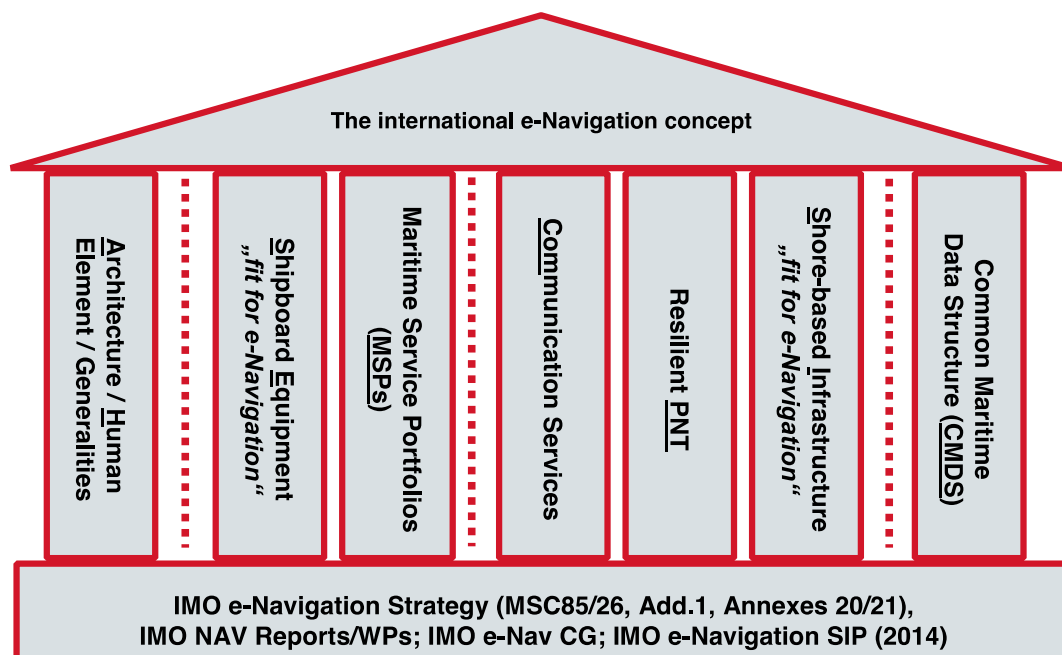


Figure 7: IMO overarching e-Navigation Architecture represented as "7 Pillars", reprinted from [1].

## 2 Review of the Potential Signals

### 2.1 The MF DGNSS Broadcast

The Milestone 2 report [3] presented methods to employ the MF DGNSS broadcasts in R-Mode. This section reviews the results presented in that report.

#### 2.1.1 Estimating the TOA

The MF DGNSS system transmits its information via a binary modulation method known as Minimum Shift Keying (MSK). Assuming that the MSK transmission is controlled by a precise time/frequency source, both the times of the bit transitions (potentially once every 10 milliseconds) and the underlying phase of the transmitted signal (a sinusoid at approximately 300 kHz) could be exploited to estimate the time of arrival (TOA) for ranging applications. The report [3] examined the potential performance of estimators of TOA from these two parameters. It was argued that with the existing signal strengths and beacons locations, the time of bit transition is too imprecise for effective ranging. However, assuming that the lane ambiguity could be resolved, the carrier phase could yield sufficient accuracy. Further, while this level of performance is conceptually possible with the direct MF transmission, it would be significantly easier if in-band CW modulations accompanied the MF and its phase was estimated. As an added benefit, producing beat frequencies from multiple CW signals could help resolve the ambiguity. For phase estimation the Cramer-Rao lower bound on accuracy is

$$\sigma_{\tau \text{ carrier}}^2 \geq \frac{1}{2\omega_c^2 T \text{ SNR}} \text{ seconds}$$

in which  $T$  is the observation period,  $\omega_c$  is the MF carrier frequency, and  $\text{SNR}$  is the received signal to noise ratio. Converting to meters and taking a square root for standard deviation

$$\sigma_{MF \text{ carrier}} \geq \frac{1.2 \times 10^4}{\omega_c \sqrt{T \text{ SNR}}} \text{ meters}$$

Figure 8 shows the potential performance (measured in meters of standard deviation) as a function of signal to noise ratio (SNR) (in dB based upon predicted signal levels and typical North Sea noise values in dBμV). The lines labelled “weak” and “typical” suggest the level of performance available in the North Sea region assuming a 5-second averaging window on the estimator.



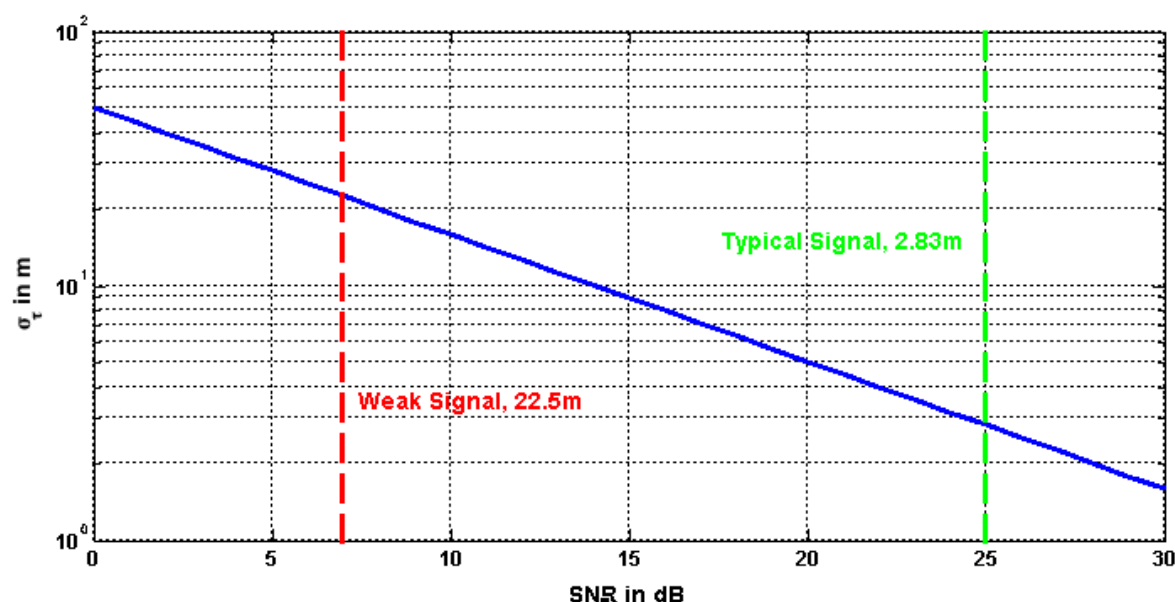


**Figure 8: The Cramer-Rao lower bound on performance of estimating the time of arrival from the phase of the MF ranging signal as a function of signal to noise ratio.**

There are several important points to remember for MF DGNSS ranging:

- Ranging using carrier phase requires the resolution of cycle ambiguity, the fact that the phase repeats every wavelength of the signal (this is approximately 1 km for MF DGNSS signals). Further, this cycle resolution is made more difficult for MSK since there is random data on the signal; hence, [3] recommended adding CW modulation to the transmission along with a pre-defined RTCM message. The pre-defined message allows for synchronization based upon the bit edges. CW allows for several ambiguity resolution approaches:
  - Initializing the receiver at a fixed location and “counting” cycles as the platform moves.
  - Using time synchronized, multiple frequency signals and solving for a position that simultaneously satisfies all of the ambiguity equations with integer solutions. This was accomplished in the Omega system by using different frequencies.
- A second point is that this performance expression is the best possible (as predicted by a Cramer-Rao bound for the additive Gaussian noise model); actual performance will be somewhat worse.
- A third point is that the propagation of an MF transmission is delayed according to the characteristics of the ground over which it is traveling. These additional secondary factors (ASFs) must be taken into account for positioning applications. While computer modelling tools can “predict” ASFs using databases of ground conductivity and topography, the quality of the prediction is typically insufficient for the desired positioning accuracy [4, 5]; the tools also do not describe the time varying nature of the ASFs. The standard solution involves surveying the area of interest to account for spatial effects based upon topography and ground conductivity and establishing monitor sites (with appropriate communications links) to provide temporal corrections to account for the time-variance in the conductivity.
- Finally, MF transmissions can suffer from multipath interference due to signal reflections off of the ionosphere; this is referred to as sky wave interference. This effect is most pronounced at night. While pulsed signals (such as Loran) can mitigate this effect, continuous transmission (as in MF) will always suffer from it.

## 2.1.2 Geometry and Signal Strength

For positioning, the quality of the solution is impacted by the signal strength and the distances and bearings to the beacon sites relative to the receiver. The signal strength is predicted using software tools and signal to noise ratio (SNR) computed by subtracting the noise for each location (described in more detail in [3]). The effect of the bearings is captured in the Horizontal Dilution of Precision (HDOP). Figure 9 shows the HDOP of the existing MF DGNSS sites for the North Sea area of interest (using only those transmitters within 500km and providing a SNR at that location of greater than 7 dB); this area is defined as region I and runs from 5°W – 15°E longitude and 50°N – 60°N latitude. Interpreted as a multiplier on the user range error in predicting the total error, lower HDOP values are better. As can be seen from this figure, most of region I has a very good (small) HDOP.

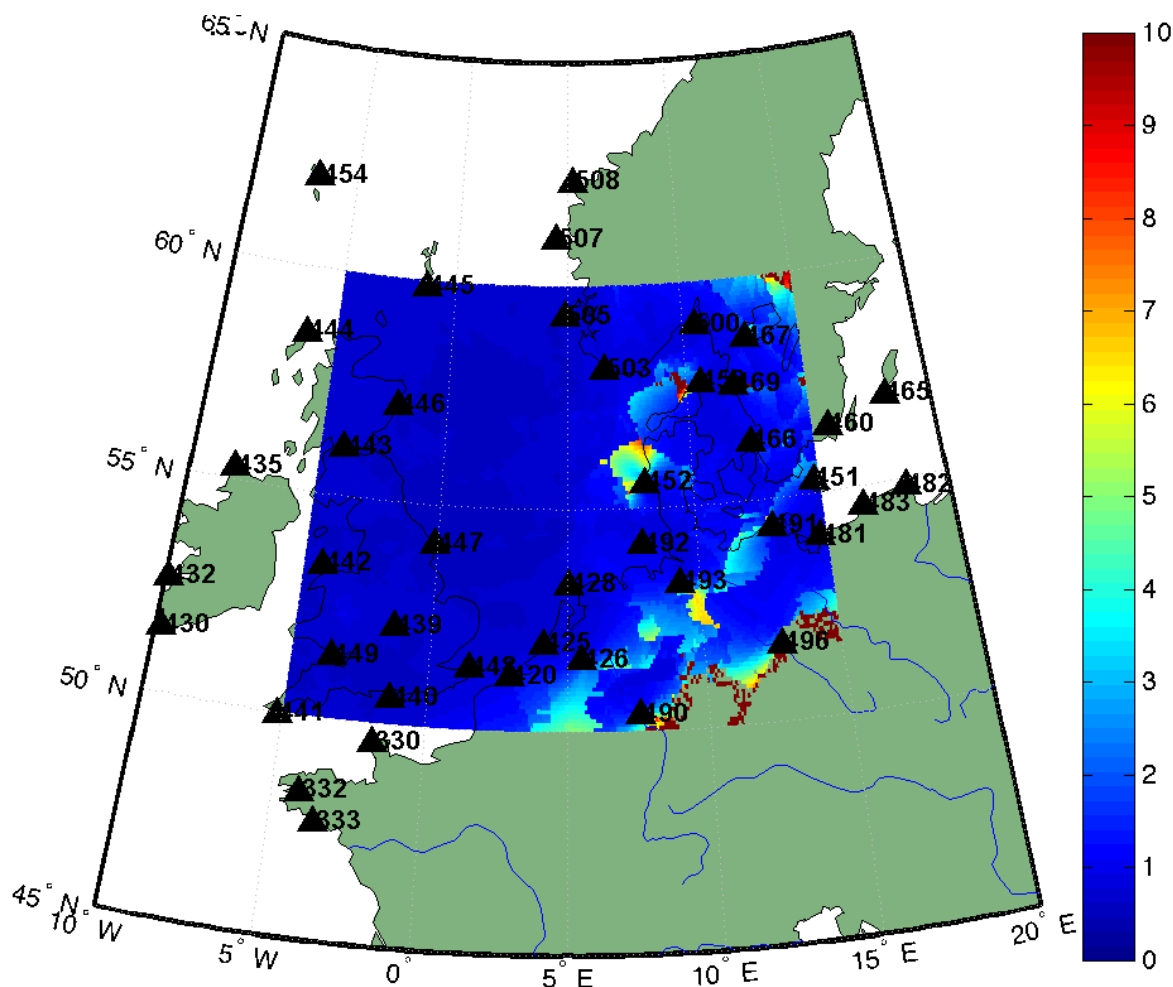
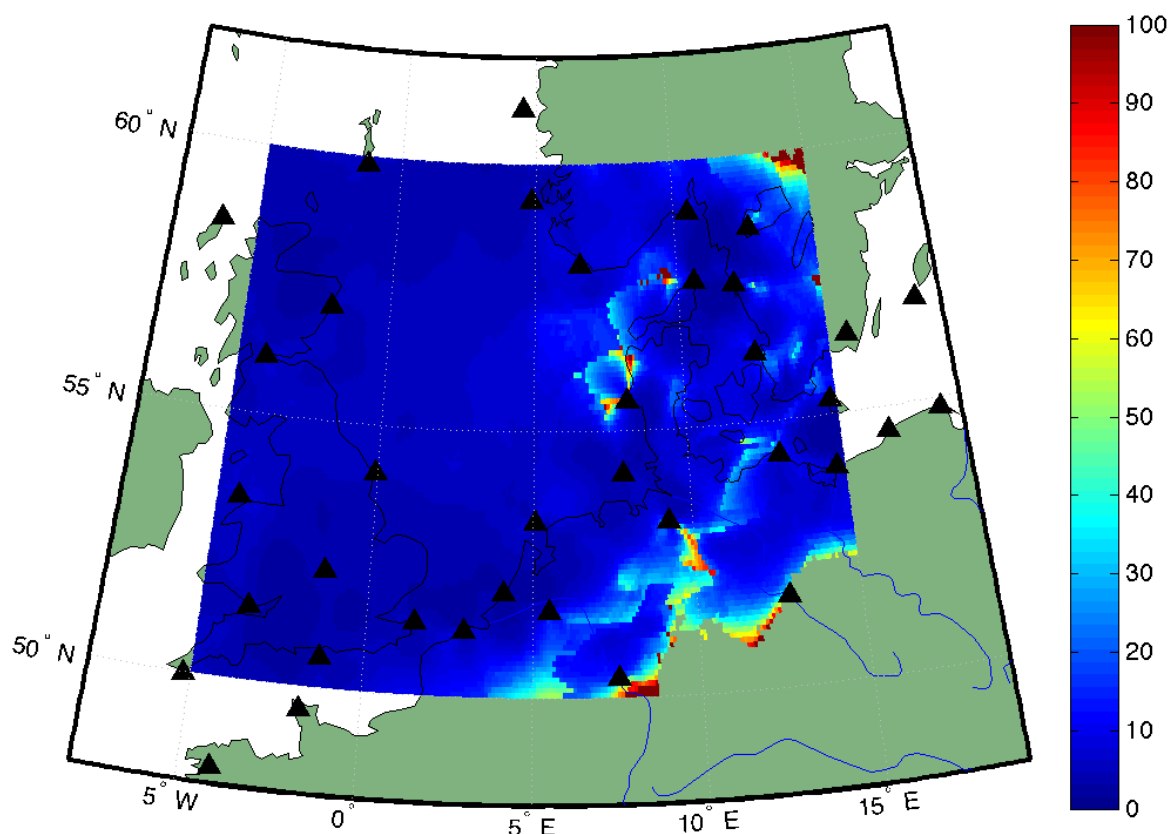


Figure 9: HDOP from the MF DGNSS sites (shown as triangles) for region I.

## 2.1.3 Positioning Accuracy

At a particular location, the pseudorange accuracy expression in 2.1.1 is evaluated using the predicted SNR at that location (computed using the method described in 2.1.2) to provide the accuracy of each individual MF DGNSS pseudorange. These accuracy values are combined with the geometry of the stations (only those with SNRs in excess of 7 dB and within 500 km) through a weighted HDOP calculation to provide a lower bound on the overall position accuracy (the general trilateration approach to computing the position and its accuracy for terrestrial RF TOA systems is described in 3.1). Figure 10 shows the result for MF DGNSS R-Mode for the North Sea area. This plot, for daytime, does not take into

account any additional errors due to timing offsets between the various transmitters (assumed perfect synchronization), nor does it take into account any secondary variations in propagation (additional secondary factors, ASFs) as these are judged to be very small over region I due to the limited land paths.



**Figure 10: Lower bound to positioning accuracy of MF DGNSS R-Mode (in meters) – day.**

As mentioned in 2.1.1 sky wave interference can have a large impact on MF DGNSS ranging performance, particularly during the night. The Milestone 2 report [3] described one method to include the effects of this interference on ranging performance by a modification of the relationship between received SNR and pseudorange accuracy. Using this result, a lower bound to positioning accuracy was developed. Figure 11 shows the result for region I; as for the daytime plot of performance, this figure ignores any additional errors due to timing offsets between the various transmitters and ASFs. Although the predicted performance shown is the lower bound mathematically, it is based on very pessimistic estimates of the sky wave impact; the actual sky wave impact could be much less and thus position accuracy better. In addition, this does not take into account any potential sky wave mitigations such as using an antenna that attenuates signals arriving from above.

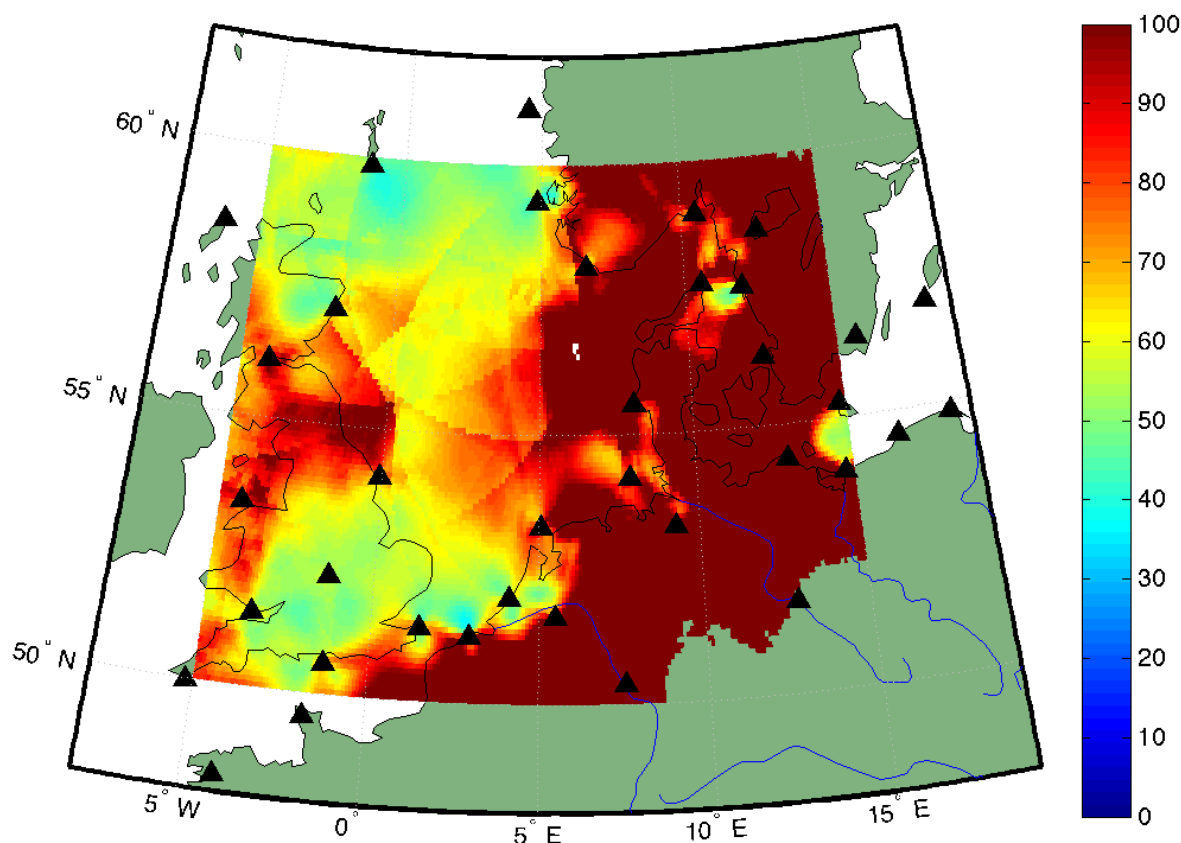


**Figure 11: Lower bound to positioning accuracy of MF DGNSS R-Mode (in meters) – night.**

### 2.1.4 R-Mode Receiver

Figure 12 contains a block diagram of an R-Mode receiver for MF DGNSS. The receiver is envisioned as an “all-in-view” system, receiving and processing as many MF DGNSS R-Mode signals as possible (shown in the figure as channels 1 through k) and using them all in the position solution:

- The DGNSS front end removes out-of-band noise and interference due to signals in the adjacent LF and AM bands. It is important that this front end not introduce time delays/phase shifts for the different DGNSS channels.
- The analog-to-digital converter (ADC) must be sufficiently fast to record the entire DGNSS band as one signal for synchronous signal processing.
- The standard MSK demodulator block estimates the bit transition times to aid in CW lane ambiguity. This receiver must also be able to decode new RTCM messages in order to receive monitor site messages for pseudorange corrections and then apply these to the pseudoranges.
- The pseudorange estimator implements standard algorithms to estimate the phases of the transmitted CW signals (in [3], we envisioned two CW signals per modulator) and resolves their ambiguity.
- An assessment of the quality of the derived pseudorange for each channel is made; specifically an assessment of the variance of the pseudorange error and, perhaps, whether or not the signal is corrupted by sky wave. Accurate assessment of this quality is required by the position solution algorithm.
- Once a sufficient number of pseudoranges are estimated (at least three for latitude, longitude, and receiver clock offset computation, but more are better), a weighted least squares position calculation is implemented. The resulting position, in the

WGS 84 datum, would be output from the receiver. Additional output information, in standard NMEA form, should include the list of stations employed in the solution, the quality of their measurements, and the receiving geometry (HDOP).

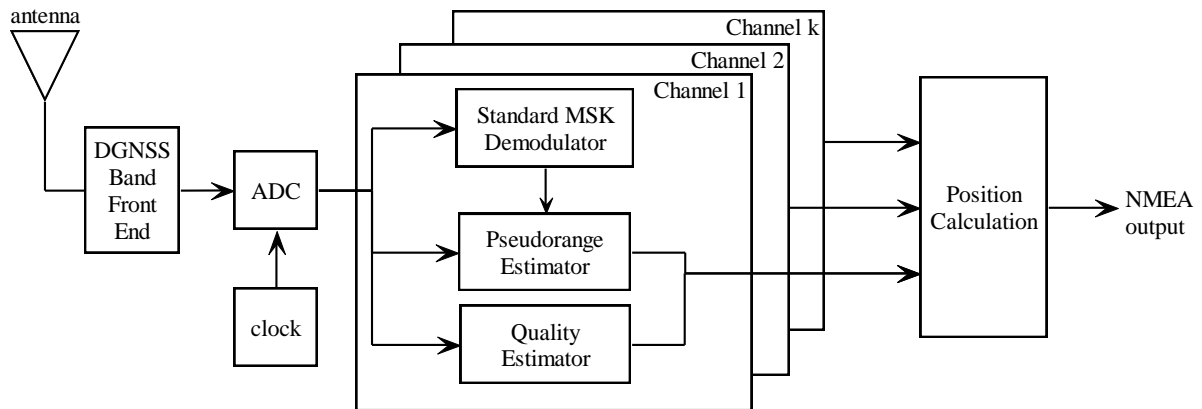


Figure 12: MF DGNSS R-Mode receiver.

## 2.2 The AIS Broadcast

The Milestone 4 report [6] presented methods to employ the AIS broadcasts in R-Mode. This section reviews the method recommended in that report.

### 2.2.1 Estimating the TOA

The AIS system transmits its information via a binary modulation method known as GMSK (Gaussian MSK), similar to MSK, but somewhat more bandwidth efficient. Assuming that the GMSK transmission is controlled by a precise timing/frequency source, both the times of the bit transitions (256 per message at a rate of 9,600 per second) and the underlying phase of the transmitted signal (a sinusoid at approximately 162 MHz) could be exploited to estimate the TOA for ranging applications. The report [6] examined the potential performance of estimators of TOA from these two parameters. It was argued that at the existing signal strengths and transmitter locations, the time of bit transition is most useful for effective ranging. The Cramer-Rao lower bound on the accuracy of the bit edge was shown to be

$$\sigma_{\tau, \text{GMSK bit edge}} \geq \frac{0.12}{\sqrt{L_0} 10^{\frac{s}{20}}} \text{ nsec}$$

Converting to meters

$$\sigma_{\tau, \text{GMSK bit edge}} \geq \frac{0.036}{\sqrt{L_0} 10^{\frac{s}{20}}} \text{ meters}$$

Figure 13 shows the potential performance (measured in meters of standard deviation) as a function of signal strength (in dBm). The lines labelled “weak” and “typical” suggest the level of performance available in the North Sea region assuming a 5-second averaging window on the estimator (assuming either five separate single-slot Message 8s or a single 5-slot Message 8).



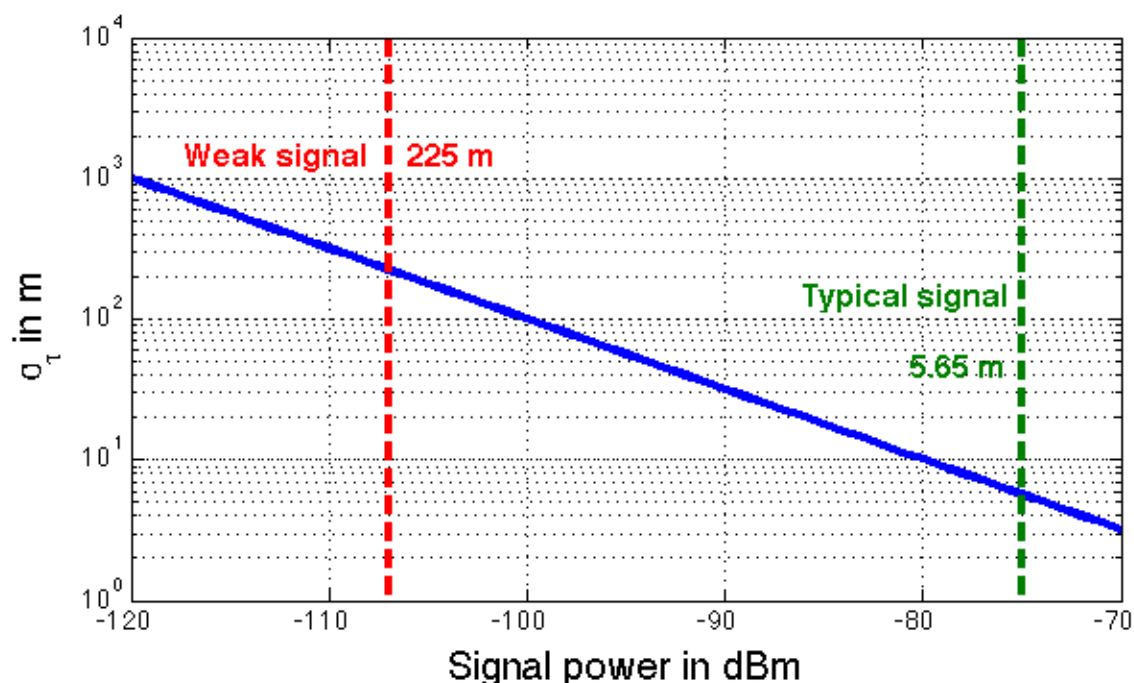


**Figure 13: The Cramer-Rao lower bound on performance of estimating the time of arrival from the AIS bit transition as a function of the received signal level in dBm.**

There are several important points to remember for AIS ranging:

- On its own, the time of a bit transition has an ambiguity of one symbol period, 26.67 msec or, in range, 31 km. Given that the propagation range for AIS for ranging is expected to be out to ~75 km, the bit transition time has limited ambiguity to resolve. For example, if the start of each AIS message is clearly aligned with a fraction of a UTC second (or some other system-wide reference), then this ambiguity is eliminated by knowledge of which bit edge it is within the message.
- A second point is that this performance expression is the best possible (as predicted by a Cramer-Rao bound for the additive Gaussian noise model); actual performance will be somewhat worse.

## 2.2.2 Geometry and Signal Strength

As mentioned in 2.1.2 the quality of the position solution is impacted by the signal strength and distances and bearings to the beacon sites relative to the receiver; the effect of the bearings is captured in the HDOP. For R-Mode AIS these sites are the AIS base stations. In [6] the area of interest was reduced from the North Sea area (20° of longitude by 10° of latitude, see Figure 9), to a smaller region to reduce the computational time; the AIS stations have a shorter range and thus there are more of them in a given area. A smaller region was selected that focuses on the high density of AIS stations along the German coast. Figure 14 shows this region (denoted II), spanning 5°-14°E longitude and 53.2°-55° N latitude, and the relevant German, Danish, and Dutch AIS base stations (shown as black squares). These form a pretty dense network of transmitters in the North and Baltic Seas and on the Kiel Canal. Signal strengths for the AIS stations were predicted using software tools (described in more detail in [6]).

Figure 14 also shows the HDOP of these AIS sites for the restricted area of interest. In computing this figure we accounted for the following:

- At VHF frequencies, the signal primarily follows a Line Of Sight (LOS) propagation path. While under certain weather conditions ducting can occur, which allows the signal to be received at distances well beyond the LOS, we have restricted our analysis to signals that travel in a normal manner and use a distance threshold of 75 km.
- Many of the German AIS stations use multiple, directional antennas to concentrate the signal energy into sectors; we take this into account as well.
- As in 2.1.2 we restrict attention to usable signals, a signal level above -117 dBm for AIS R-Mode.

As can be seen from this figure, most of the study area has a very good (small) HDOP.

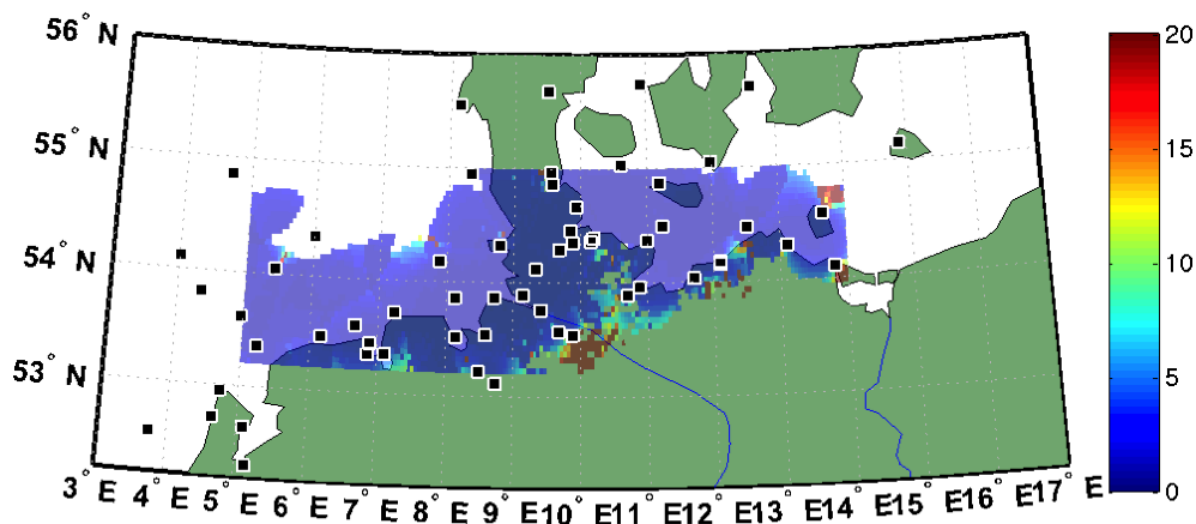


Figure 14: HDOP for the AIS base stations (shown as squares) in region II.

### 2.2.3 Positioning Accuracy

At a particular location, the pseudorange accuracy expression in 2.2.1 is evaluated using the predicted signal level at that location (computed using the method described in 2.2.2) to provide the accuracy of each individual AIS pseudorange. These accuracy values are combined with the geometry of the stations (only those with signal strengths in excess of -117 dBm and within 75 km) through a weighted HDOP calculation to provide a lower bound on the overall position accuracy (the general trilateration approach to computing the position and its accuracy for terrestrial RF TOA systems is described in 3.1). Figure 15 shows the result for AIS R-Mode in region II. As above, this plot does not take into account any additional errors due to timing offsets between the various transmitters (assumed perfect synchronization), nor does it take into account any multipath or other interference, only additive white Gaussian noise. For this analysis, 60 slots per minute (or one 256 bit slot per second) and a receiver averaging time of 5 seconds for a total of 1,280 bits is used.

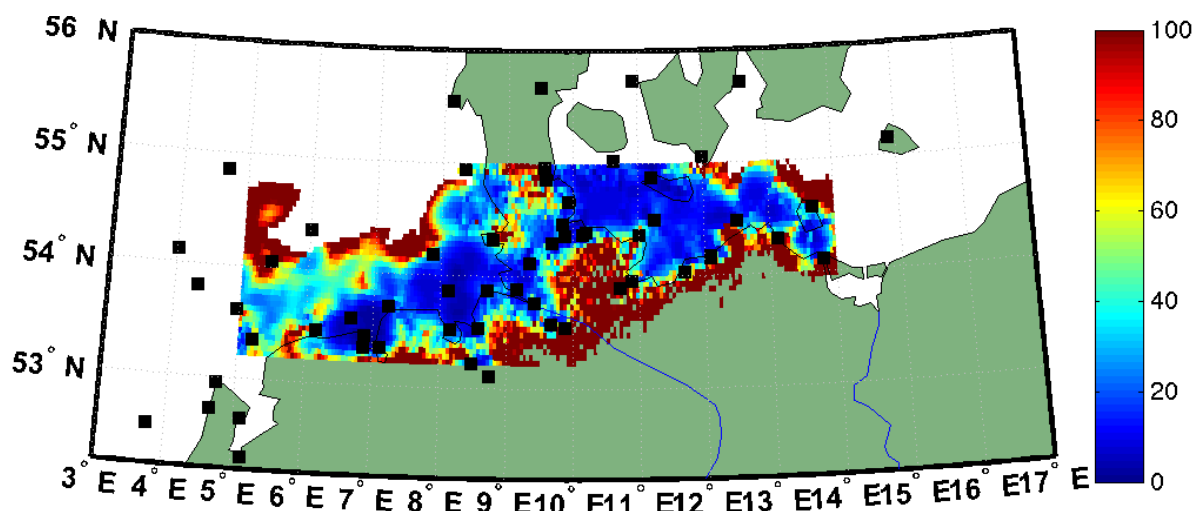


Figure 15: Lower bound to positioning accuracy of AIS R-Mode (in meters) in region II (AIS stations shown as black squares).

## 2.2.4 R-Mode Receiver

Figure 16 contains a block diagram of an all-in-view AIS R-Mode receiver to implement ranging from existing AIS signals; it consists of the following:

- The AIS front end/mixer removes out-of-band noise and interference and converts the VHF signal to an intermediate frequency (this could be baseband).
- The analog-to-digital converter (ADC) samples the signal for digital processing.
- The AIS pseudorange estimator block implements algorithms to estimate the pseudorange from the time of bit transitions. The output of this block is the estimated pseudorange and an estimate of its error variance (for weighting in the position solution). Note that this block, one for each AIS channel, processes AIS signals from all AIS base stations visible. Since these are transmitting in separate time slots, there is no overlap of processing.
- Once a sufficient number of pseudoranges are estimated (at least three for latitude, longitude, and receiver clock offset computation, but more are better), a weighted least squares position calculation is implemented. The resulting position, in the WGS 84 datum, would be output from the receiver. Additional output information, in standard NMEA form, should include the list of stations employed in the solution, the quality of their measurements, and the receiving geometry (HDOP).

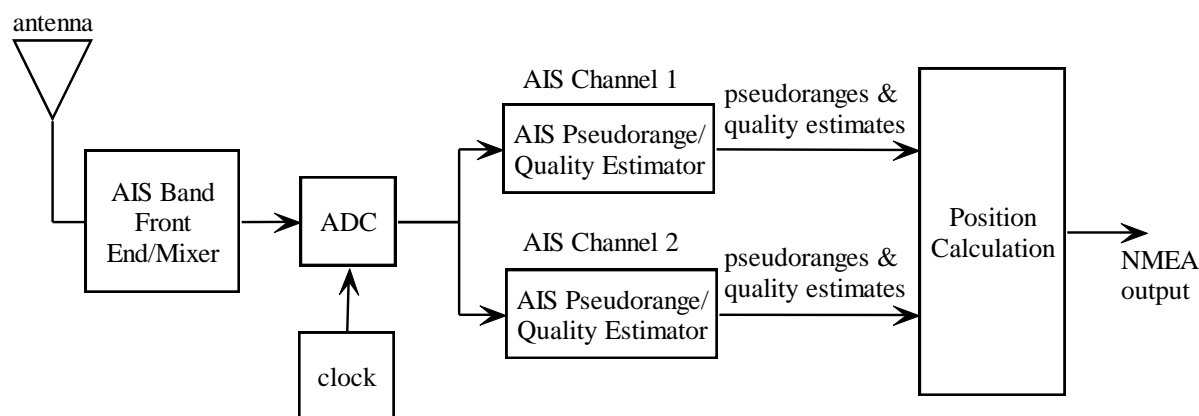


Figure 16: AIS R-Mode receiver.

## 2.3 eLoran

### 2.3.1 Estimating the TOA

Loran is a pulsed ranging system with a long history (see, for example, the years of proceedings of the Wild Goose Association and the International Loran Association). In [7] we examined the ranging performance of a typical Loran receiver as a function of the received signal strength (as measured at the third zero crossing). Figure 17, reprinted from [7], yielded an approximation to the accuracy of

$$\sigma_{Loran} \approx \sqrt{10^{\frac{123-SS}{10}} + \sigma_{jitter}^2} \text{ nsec}$$

in which SS is the signal strength in units of dBμV and  $\sigma_{jitter} = 60$  or 90 nsec for a single or dual rated transmitter respectively (note that the referenced paper contained an error, replacing the constant 123 by 13).

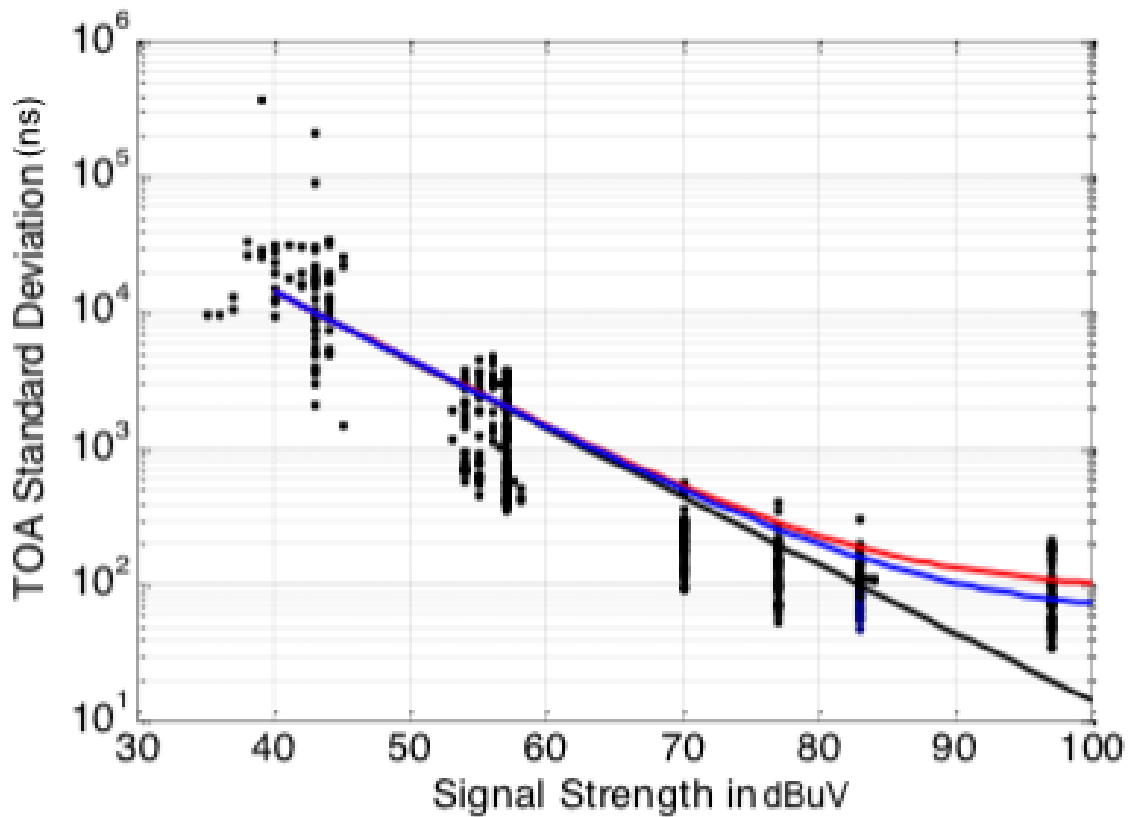


**Figure 17: Typical performance of estimating the time of arrival from the eLoran signal as a function of the received signal strength in dBμV (reprinted from [7]).**

This expression is for a single received Loran pulse and must be scaled by the number of pulses averaged for the TOA estimate. As the scaling is reciprocal and follows the square root of the number of pulses, the equivalent expression would be

$$\sigma_{TOA} \approx \sqrt{\frac{10^{\frac{123-SS}{10}} + \sigma_{jitter}^2}{\text{number of pulses averaged}}} \text{ nsec}$$

Finally, converting to meters (0.3 meters per nsec)

$$\sigma_{TOA} \approx 0.3 \sqrt{\frac{\frac{123-SS}{10 \cdot 10} + \sigma_{jitter}^2}{\text{number of pulses averaged}}} m$$

For example, the dual rated Loran transmitter at Sylt transmits on two GRIs (Group Repetition Intervals), 6731 and 7499. In a 5-second period this is a total of approximately 1127 pulses (5 seconds  $\times$   $10^6/67310$  groups per second  $\times$  8 pulses per group = 594 pulses for the 6731 rate plus another 533 for the 7499 rate) of which a percentage are lost to blanking (for computational purposes, we assume that 10% of the second rate pulses are blanked). So

$$\sigma_{TOA,Sylt} \approx 0.3 \sqrt{\frac{\frac{123-SS}{10 \cdot 10} + 90^2}{1127 \times 0.9}} m$$

There are several important points to remember for eLoran ranging:

- Similar to the MF DGNSS signal, the Loran signal is delayed by the characteristics of the ground over which it is traveling. These ASFs must be taken into account for positioning applications. Limited ASF maps have been generated for the Loran stations considered here; primarily for the Harwich harbour area, for example see [8].
- Loran receivers can suffer from multipath interference due to signal reflections off of the ionosphere (sky wave interference). This effect is most pronounced at night and at long distances. The Loran pulses have been designed to mitigate this interference and at the shorter ranges considered here, these effects are negligible.



### 2.3.2 Geometry and Signal Strength

As already mentioned in 2.1.2 the quality of the position solution is impacted by the signal strengths and distances and bearings to the transmitter sites relative to the receiver; the effect of the bearings is captured in the HDOP. For eLoran in the North Sea area there are five relevant eLoran sites: Sylt, Lessay, Anthorn, Ejde, and Vaerlandet. Figure 18 shows the transmitter geometry with respect to the MF DGNSS evaluation area (the larger box covering the North Sea, region I) and the AIS evaluation area (the smaller, inset box including Sylt, region II) and an even smaller area around the Kiel Canal and Elbe River, region III which covers from 8.5°E – 10.5°E longitude and 53.4°N – 54.5°N latitude. The three proposed test bed areas (discussed in Section 3.5) are also shown: test bed 1 in red, test bed 2 in black (same as region III) and test bed 3 in blue.

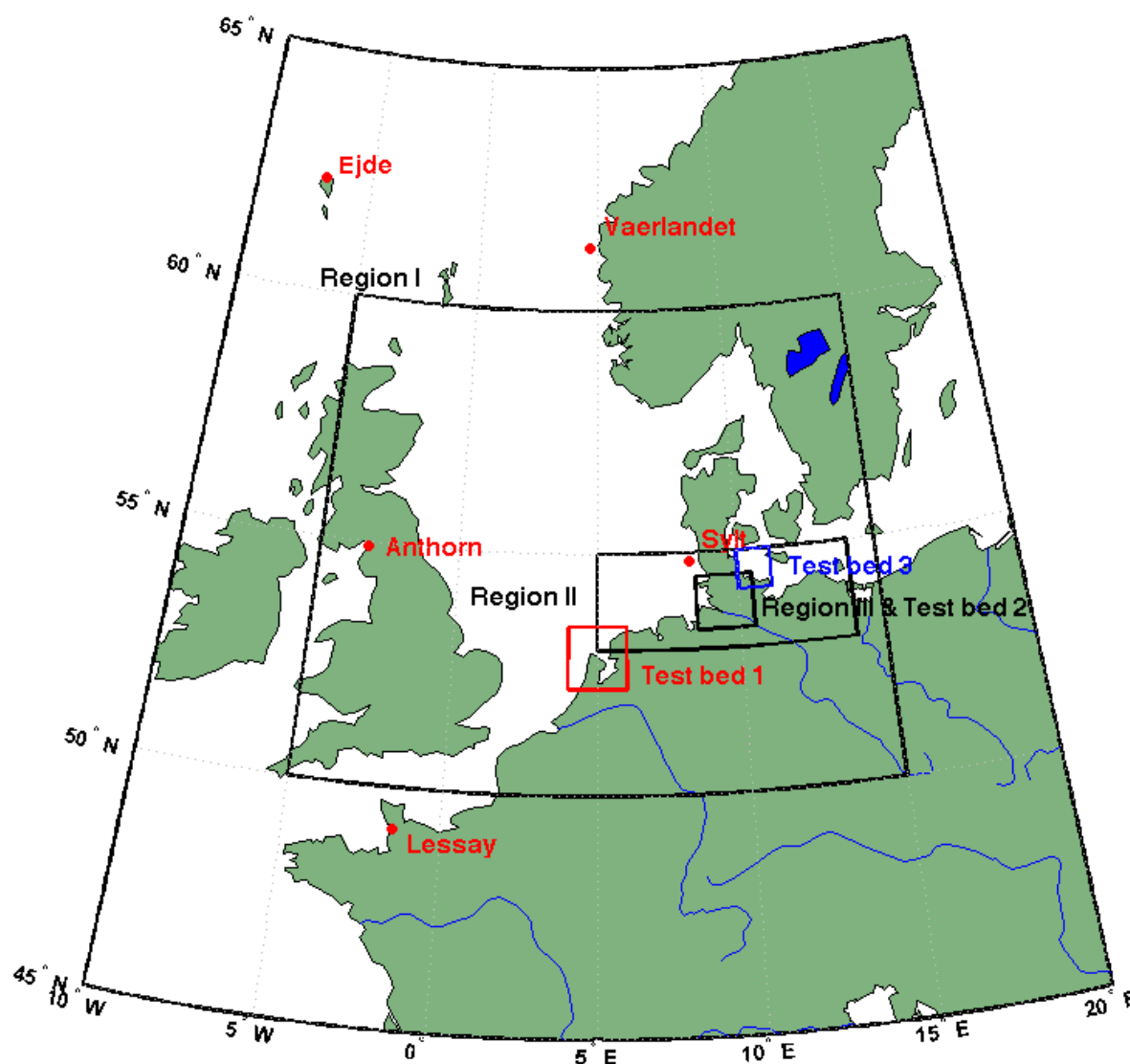
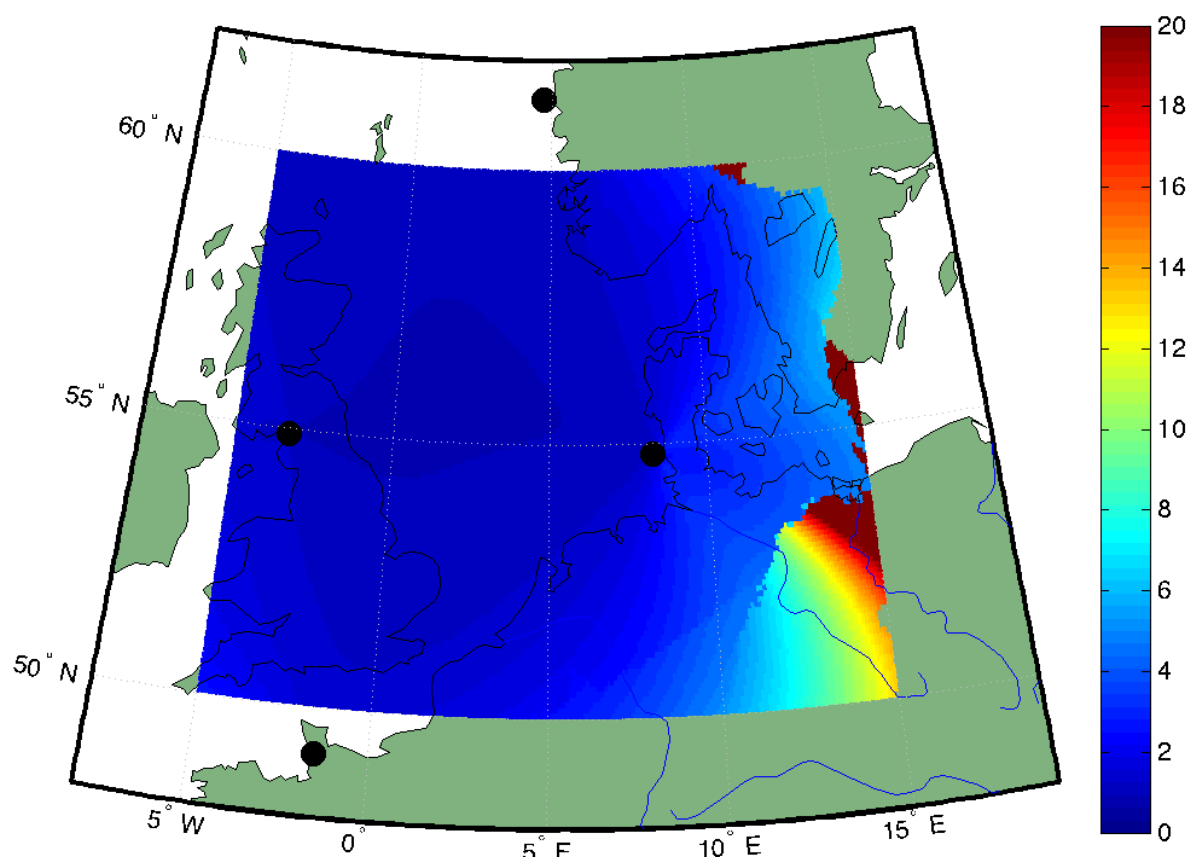


Figure 18: eLoran transmitter locations (shown as red dots) relevant to the regions of interest (I, II, and III) and test beds (1, 2, and 3).

Figure 19 shows the HDOP of these eLoran sites for the areas of interest. In computing this figure we restrict inclusion to strong signals, above 50 dB $\mu$ V. As can be seen from this figure, the area within triads of eLoran towers has a very good (small) HDOP; to the east of Sylt the HDOP falls off dramatically.



**Figure 19: HDOP for the five eLoran stations in region I); Loran towers marked with black circles (Ejde is located to the NW just off the plot).**

The typical method to predict loss of signal power with distance is to use software tools. For the eLoran assessment in this report, signal strengths were provided by the General Lighthouse Authorities of the UK and Ireland for region I. A sample signal strength plot, for the Sylt transmitter, is shown in Figure 20. Although not shown, as it lies outside the region I boundary, the signal coverage from Sylt extends much farther to the East which could be used along with the MF sites around the Baltic.

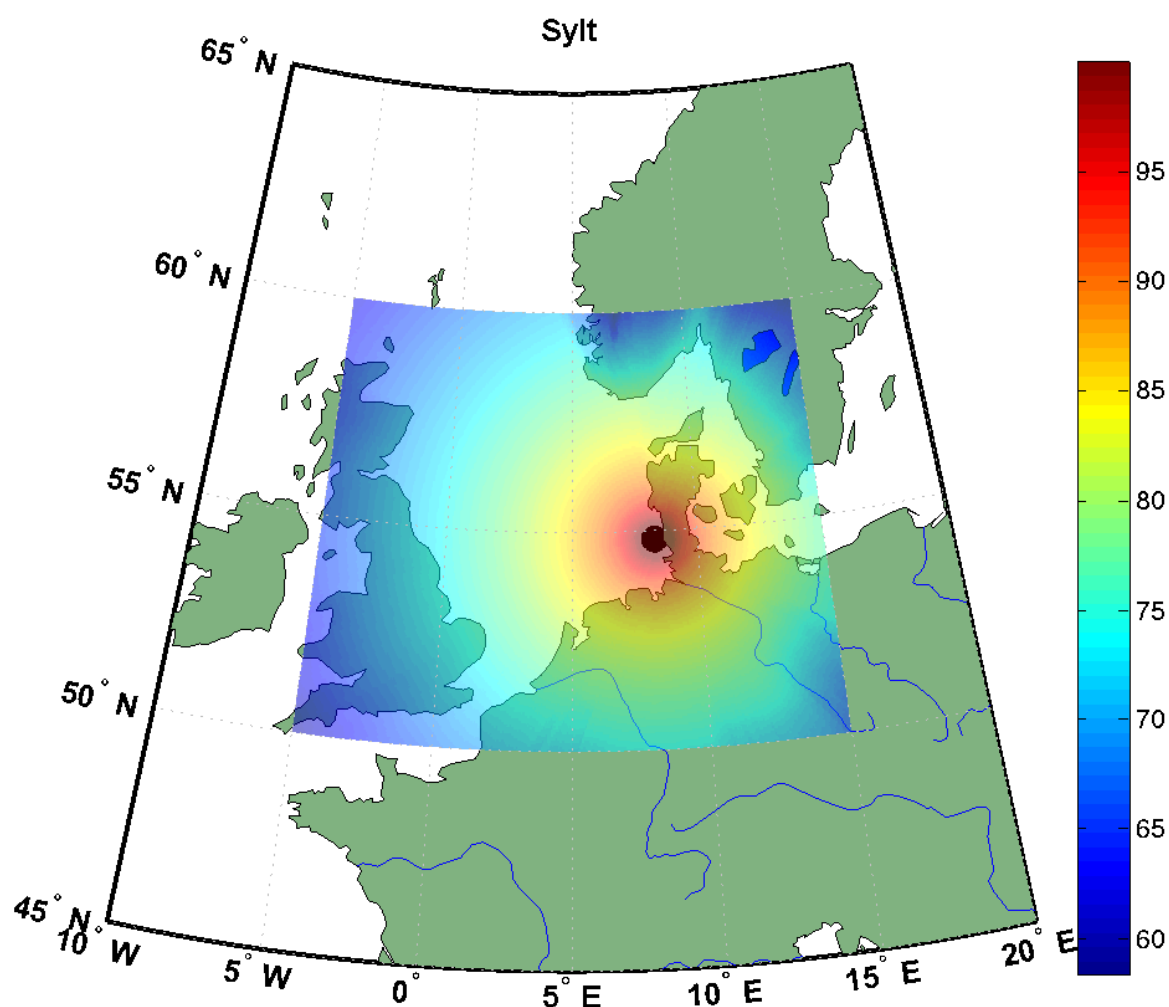
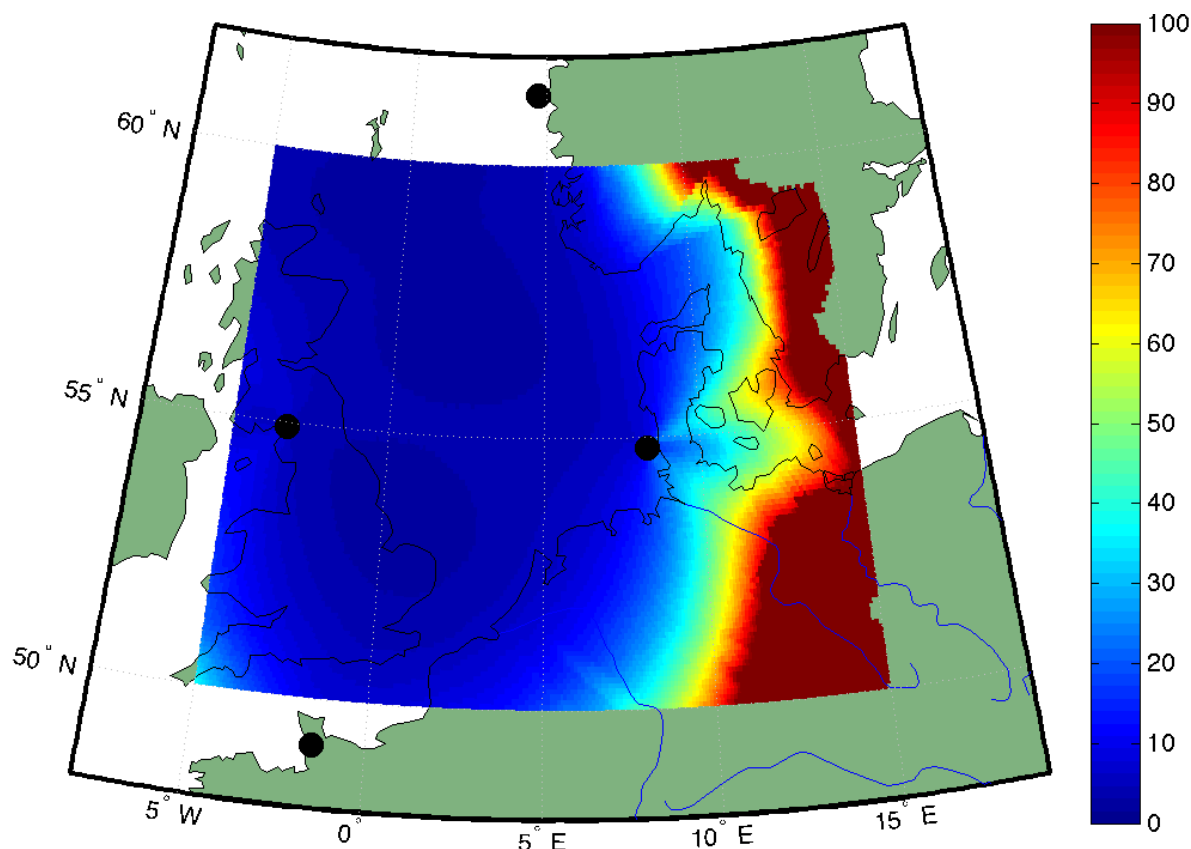


Figure 20: Predicted signal strength for a typical eLoran site, Sylt (in dBμV); Sylt is indicated by the black circle.

### 2.3.3 Positioning Accuracy

At a particular location the pseudorange accuracy expression in 2.3.1 is evaluated using the predicted signal strength at that location (acquired as described in 2.3.2) to provide the accuracy of each individual eLoran pseudorange. These accuracy values are combined with the geometry of the stations (only those with signal strengths in excess of 50 dBμV) through a weighted HDOP calculation to provide a lower bound on the overall position accuracy (the general trilateration approach to computing the position and its accuracy for terrestrial RF TOA systems is described in 3.1). Figure 21 shows the result for eLoran for region I. This plot does not take into account any additional errors due to timing offsets between the various transmitters (assumed perfect synchronization) nor does it take into account ASFs.

We note that much of region I is within the area of the triangles formed by the five Loran tower locations; hence, the positioning performance on that area is quite good (sub 20 meters on this scale). Moving to the East we lose signals; hence, the rapid degradation in performance. At the very Eastern end of the region of interest, in the North and South corners, we have fewer than the required three signals to compute a position.



**Figure 21: Lower bound to positioning accuracy of eLoran (in meters); Loran towers marked with black circles (Ejde is located to the NW just off the plot).**

It is very possible that both Norway and France will discontinue eLoran operations at their sites; if this were to happen then eLoran positioning would NOT be possible in the North Sea area (signals from at least three separate transmitters are needed to compute latitude and longitude). If Norway were to discontinue operations but France kept Lessay, then eLoran positioning would still be possible in the southern part of the North Sea. Figure 22 shows the predicted performance using just these three Loran towers (Sylt, Anthorn, and Lessay).

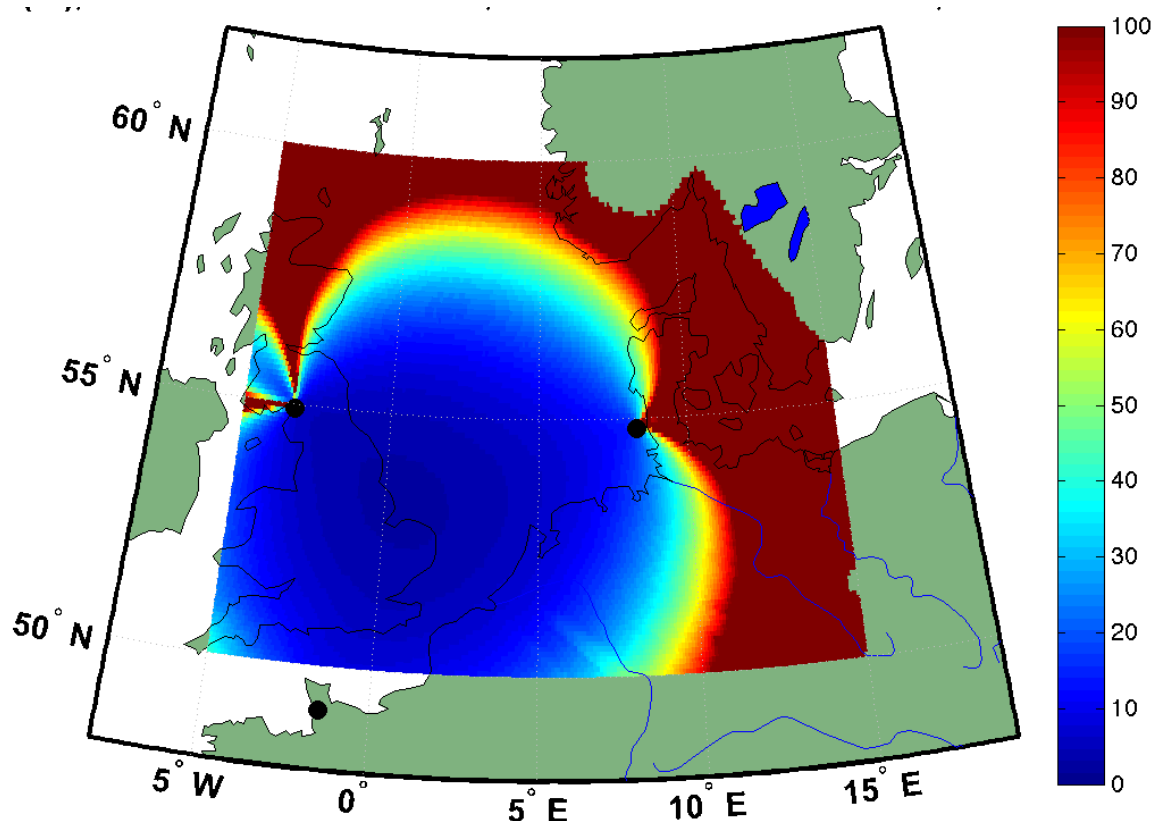


Figure 22: Lower bound to positioning accuracy of eLoran (in meters) with just three stations; Loran towers marked with black circles.

### 2.3.4 eLoran Receiver

eLoran receivers have received much attention in the last 15 years as part of the United States Loran-C recapitalization process (see, e.g., [9-14]). Figure 23 contains a generic block diagram of an eLoran receiver. This receiver is envisioned as an “all-in-view” system, receiving and processing as many eLoran signals as possible (shown in the figure as channels 1 through k) and using them all in the position solution:

- The eLoran front end/mixer removes out-of-band noise and interference.
- The analog-to-digital converter (ADC) samples the signal for digital processing.
- The pseudorange/quality estimator block implements algorithms to estimate the pseudorange from the individual eLoran pulses. The output of this block is the estimated pseudorange and an estimate of its error variance (for weighting in the position solution). Note that this block, one for each eLoran station being tracked channel, processes pulses for that specific station only (by separating pulses in time and averaging).
- Once a sufficient number of pseudoranges are estimated (at least three for latitude, longitude, and receiver clock offset computation, but more are better), a weighted least squares position calculation is implemented. The resulting position, in the WGS 84 datum, would be output from the receiver. Additional output information, in standard NMEA form, should include the list of stations employed in the solution, the quality of their measurements, and the receiving geometry (HDOP).



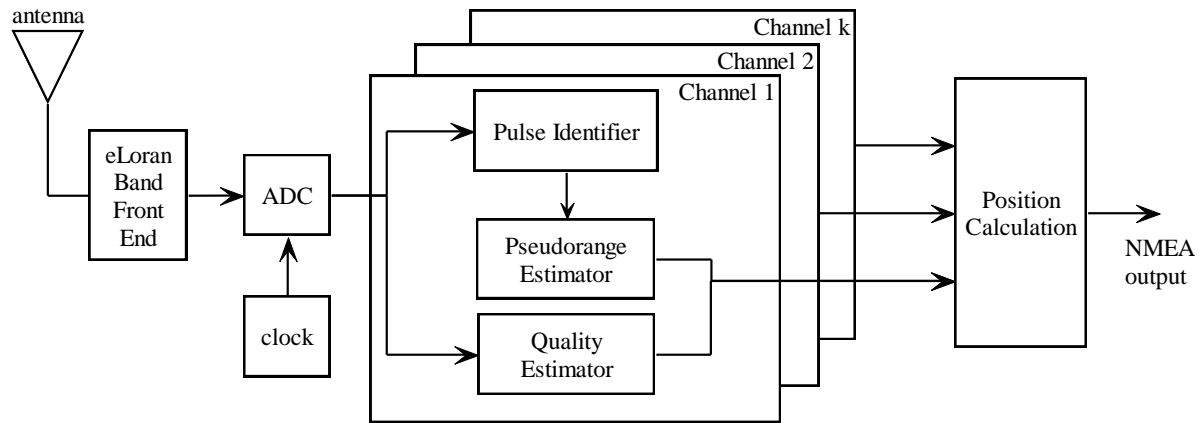


Figure 23: eLoran receiver.

### 3 Combining Ranging Signals

#### 3.1 The Truly “All-in-View” Receiver

The position solution (actually position and clock offset) from radionavigation TOA observables does not, in general, have a closed form solution. The usual approach is to assume some approximate position and iteratively solve a linearized version of the problem. For terrestrial systems (such as Loran) this is typically a weighted least squares solution with error weights dependent upon the accuracy of the individual TOA measurements [15]. Assuming  $n$  transmitters, at azimuth angles  $\varphi_k$  with respect to the assumed position, the linearized equations are [15]

$$\begin{bmatrix} \sin \varphi_1 & \cos \varphi_1 & 1 \\ \sin \varphi_2 & \cos \varphi_2 & 1 \\ \vdots & \vdots & \vdots \\ \sin \varphi_n & \cos \varphi_n & 1 \end{bmatrix} \begin{bmatrix} \delta x \\ \delta y \\ c\delta t \end{bmatrix} = c \begin{bmatrix} \delta TOA_1 \\ \delta TOA_2 \\ \vdots \\ \delta TOA_n \end{bmatrix}$$

in which  $\delta x$ ,  $\delta y$ , and  $\delta t$  are the differentials in the  $x$  and  $y$  position and clock offset solutions, respectively (relative to the assumed solution),  $c$  is the speed of light, and each  $\delta TOA_k$  is the differential in the TOA measurement. It is common to write this in set of equations in matrix form as

$$\mathbf{A}\delta = \mathbf{z}$$

defining the direction cosines matrix ( $\mathbf{A}$ ), the vector of differential TOAs ( $\delta$ ) and the position/clock differential vector ( $\mathbf{z}$ ). The HDOP is defined by first computing

$$\mathbf{H} = (\mathbf{A}^T \mathbf{A})^{-1}$$

and then

$$HDOP = \sqrt{H_{1,1} + H_{2,2}}$$

Assuming independent TOA measurements, the covariance matrix of  $\mathbf{z}$  is

$$\mathbf{R} = \begin{bmatrix} \sigma_1^2 & 0 & \dots & 0 \\ 0 & \sigma_2^2 & \dots & 0 \\ \vdots & \vdots & \ddots & \vdots \\ 0 & 0 & \dots & \sigma_n^2 \end{bmatrix}$$

(i.e. white noise with variances  $\sigma_k^2$  on the  $k^{\text{th}}$  TOA measurement), the weighted least squares solution using weight matrix  $\mathbf{R}^{-1}$  is

$$\delta = (\mathbf{A}^T \mathbf{R}^{-1} \mathbf{A}) \mathbf{A}^T \mathbf{R}^{-1} \mathbf{z}$$

which has error covariance (a 3-by-3 result)

$$\mathbf{G} = (\mathbf{A}^T \mathbf{R}^{-1} \mathbf{A})^{-1}$$

The weighted HDOP (skipping the variance of the clock offset solution,  $G_{3,3}$ ) is found as

$$\sigma_{\text{position}} = \sqrt{G_{1,1} + G_{2,2}}$$

Hence, to measure performance at a particular location, we need to know which signals are available, the geometry to the signals, and what their accuracies are.

Assuming that all observable signals are synchronized at transmission, there is no need to limit the measurements to being from one type of source. We can combine measurements from multiple sources as long as we have estimates of their individual accuracies (in the same units) and angles to the transmitters. Specifically, angles  $\varphi_k$ , differential measurements  $\delta TOA_k$ , and variances  $\sigma_k^2$  could come from MF DGNSS for  $k = 1, 2, \dots, n_1$ , from AIS for  $k = n_1 + 1, \dots, n_2$ , and from eLoran for  $k = n_2 + 1, \dots, n$ .

Note that the addition of new measurements from additional transmitters cannot increase the HDOP or weighted HDOP. At worst (and this occurs if the new transmitter's location is at the same azimuth as a current transmitter), the HDOP and weighted HDOP stay the same [16].

Figure 24 contains a block diagram of such a combined signal, “all-in-view” R-Mode receiver. It essentially combines the separate MF, AIS, and eLoran receivers already described (Figure 12, Figure 16, and Figure 23) with a common “position calculation” block implementing the algorithm just described. For simplicity the diagram shows three distinct antennae although eLoran and MF DGNSS could potentially share an antenna due to their closeness in frequency.

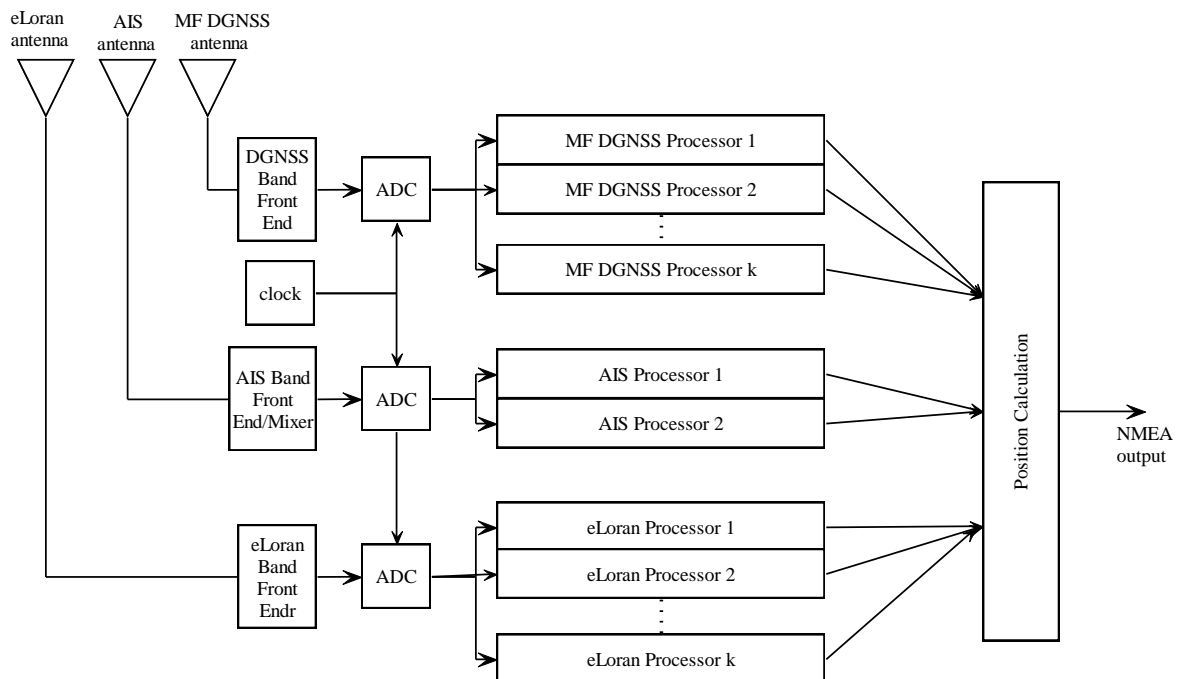


**Figure 24: MF+AIS+eLoran “All-in-View” R-Mode receiver.**

### 3.2 MF DGNSS and eLoran

For a first example of combined performance, consider MF DGNSS R-Mode plus eLoran on the full North Sea area, region I. Accuracies for MF DGNSS R-Mode and eLoran alone are shown in Figure 10 (MF DGNSS-day), Figure 11 (MF DGNSS-night), and Figure 21 (eLoran). Since the performance of both eLoran and MF DGNSS alone during the day is good; we have presented the combination only for the night when MF DGNSS performance alone is greatly reduced (see Figure 25). The addition of eLoran improves performance of the night time MF DGNSS considerably. The addition of MF DGNSS to eLoran improves performance in the western Baltic Sea area and allows for position solutions in the Northeast and Southeast corners of region I. Although not shown, as it lies outside the region I boundary, the signal coverage from Sylt extends much farther to the East which could be used along with the MF DGNSS sites around the Baltic.

If France and Norway do shut down their Loran stations then it becomes impossible to do an eLoran solution in the North Sea. However, the addition of one or two Loran stations to the solution can improve MF DGNSS performance considerably at night; see Figure 26 for the night performance using just Sylt and Figure 27 for the night performance using both Sylt and Anthorn. The coverage “hole” seen at night in the middle of the region can be partially filled by adding in Ekofisk as discussed in the Milestone 2 report (see Figure 28). As mentioned in Section 2.1, the MF DGNSS performance at night is strongly impacted by sky wave, the model we have used to model this error is pessimistic, so performance could be better in reality.

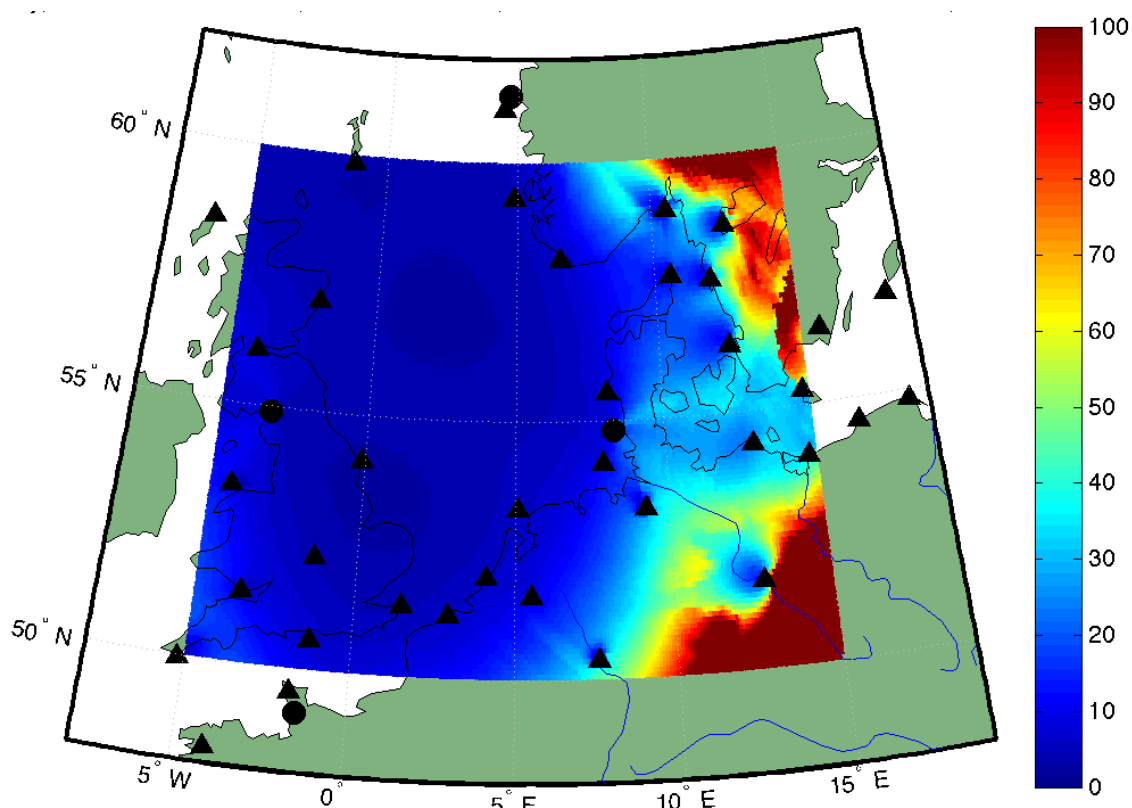


**Figure 25: Lower bound to positioning accuracy of combined MF DGNSS R-Mode and eLoran on region I – night.**

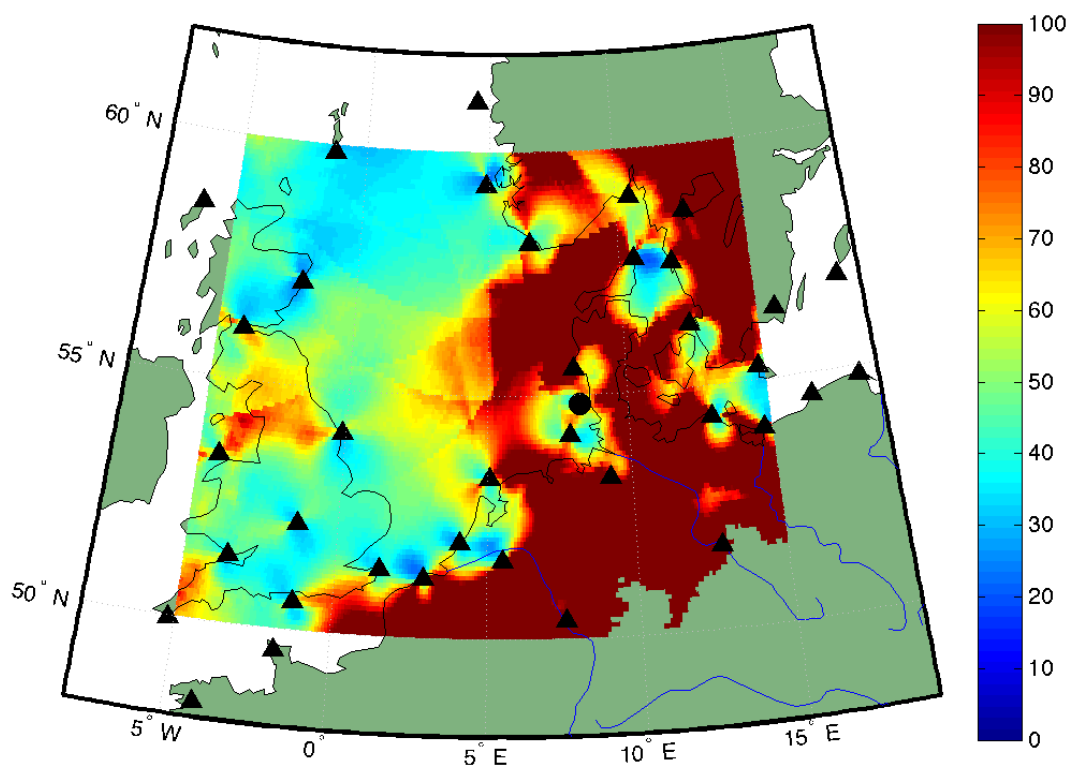


**Figure 26: Lower bound to positioning accuracy of combined MF DGNSS and eLoran (Sylt only) on region I – night.**

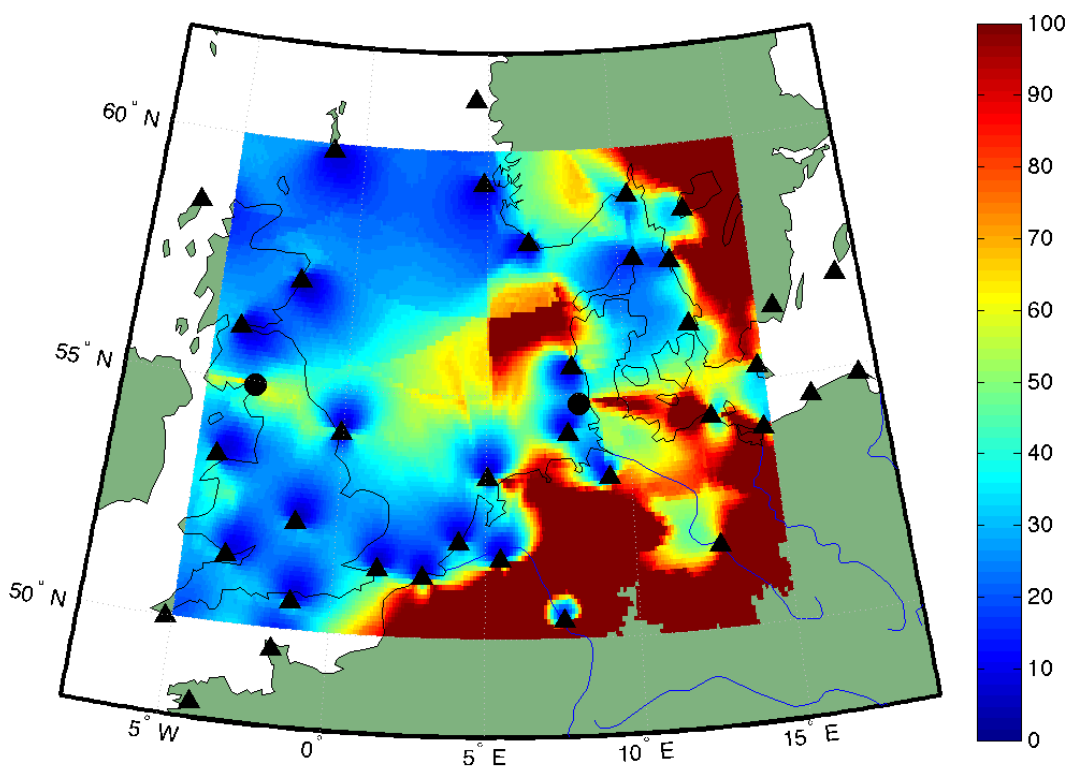


**Figure 27: Lower bound to positioning accuracy of combined MF DGNSS and eLoran (Sylt and Anthorn) on region I - night.**

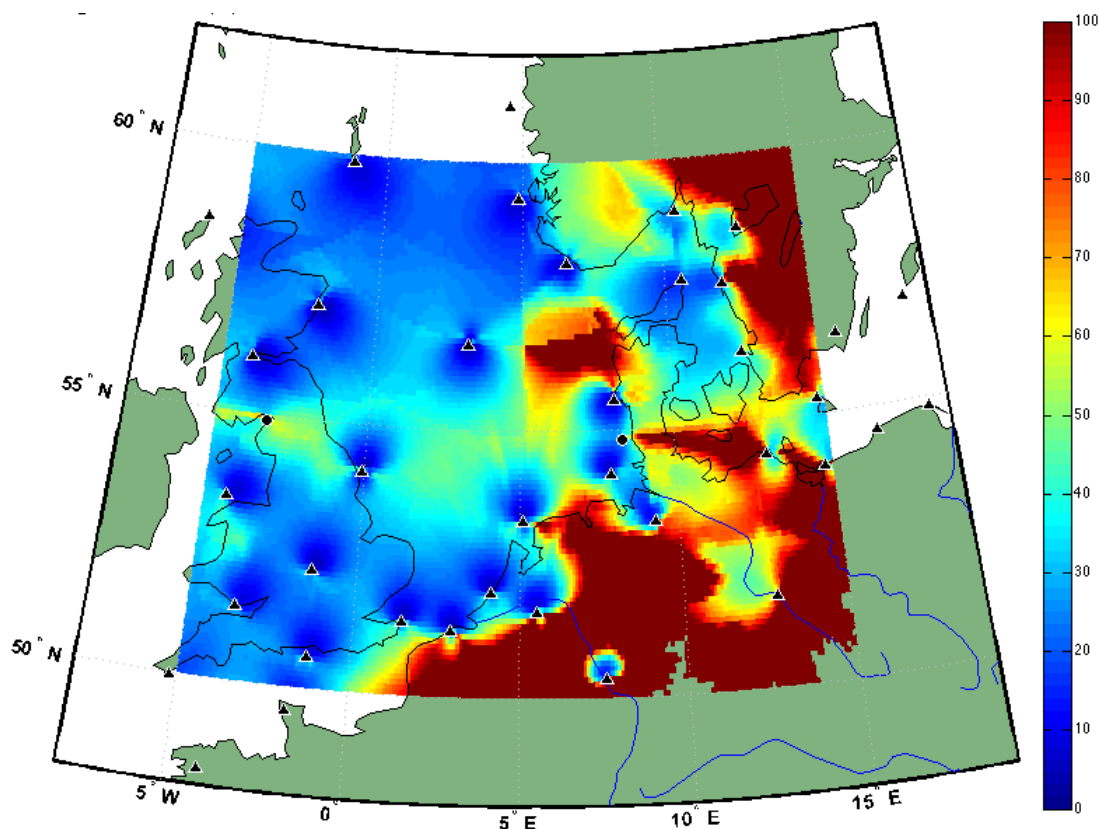


**Figure 28: Lower bound to positioning accuracy of combined MF DGNSS and eLoran (Sylt and Anthorn) on region I – night with Ekofisk added.**

We note the following in this example:

- During the day the performance of MF DGNSS R-Mode is great; there is very little improvement seen by adding eLoran ranges. Except, as noted above, MF DGNSS R-Mode requires a solution for cycle ambiguity; reception of even a single eLoran signal can assist with this ambiguity resolution.
- eLoran (the full system) is already quite effective in this region by itself so there is little improvement seen by adding MF DGNSS (especially at night when MF DGNSS performance is worse than the day). The primary aid is to the east where eLoran coverage is limited.
- If eLoran is reduced to only 1 or 2 towers then an eLoran solution is not possible. However, adding only 1 or 2 towers to MF DGNSS can improve MF DGNSS performance considerably at night.
- There has been some discussion in the industry for a low-power Loran system that might be lower cost; this is not needed in the North Sea area as Sylt and Anthorn are available and if additional sites are needed for HDOP reasons, then it is probably cheaper to install additional MF DGNSS sites.

### 3.3 MF DGNSS and AIS

For a second assessment of combining R-Mode signals, consider a joint MF DGNSS/AIS receiver. As the examination of AIS R-Mode alone (in [6]) restricted attention to areas near the German AIS network (region II), including the German bight, this example focuses on combined performance in that area.

To assess performance we consider both day and night conditions (due to the effects of sky wave interference on MF DGNSS at night). Figure 15 showed the performance of AIS R-Mode alone. The lack of coverage in the northwest and southeast is apparent; the fringes of these areas, with only 3 nearby transmitters, exhibit poor positioning performance. The central region of this figure, with many AIS transmitters visible, sees better performance. Figure 10 and Figure 11 showed the performance of MF DGNSS R-Mode alone for region I, day and night, respectively. Figure 29 and Figure 30 zoom in on these figures for region II. The accuracy of MF DGNSS alone during the day is good over the majority of region II; at night, sky wave interference severely reduces performance.

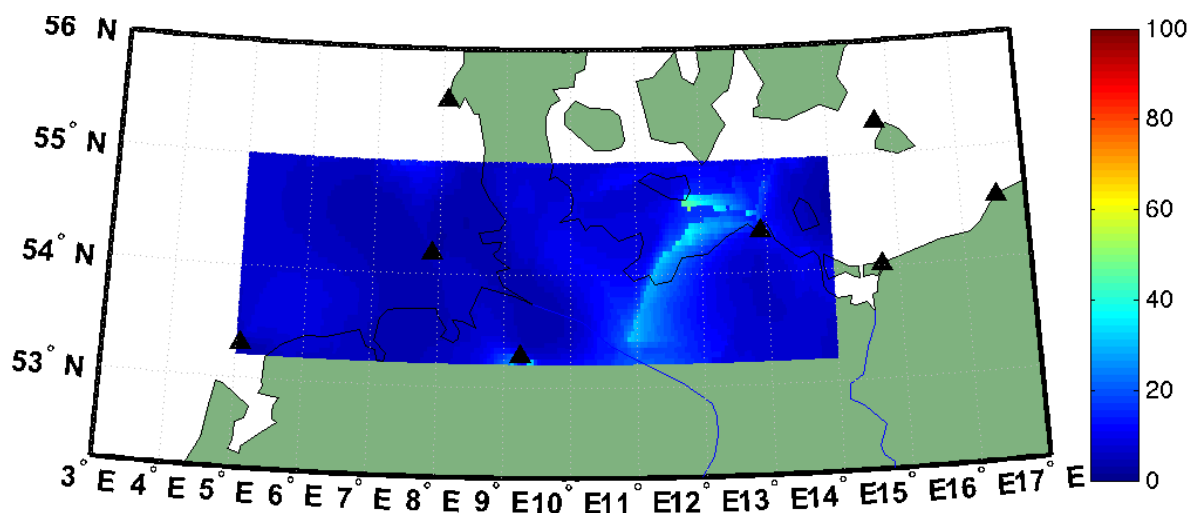


Figure 29: Lower bound to positioning accuracy of MF DGNSS R-Mode on region II – day.

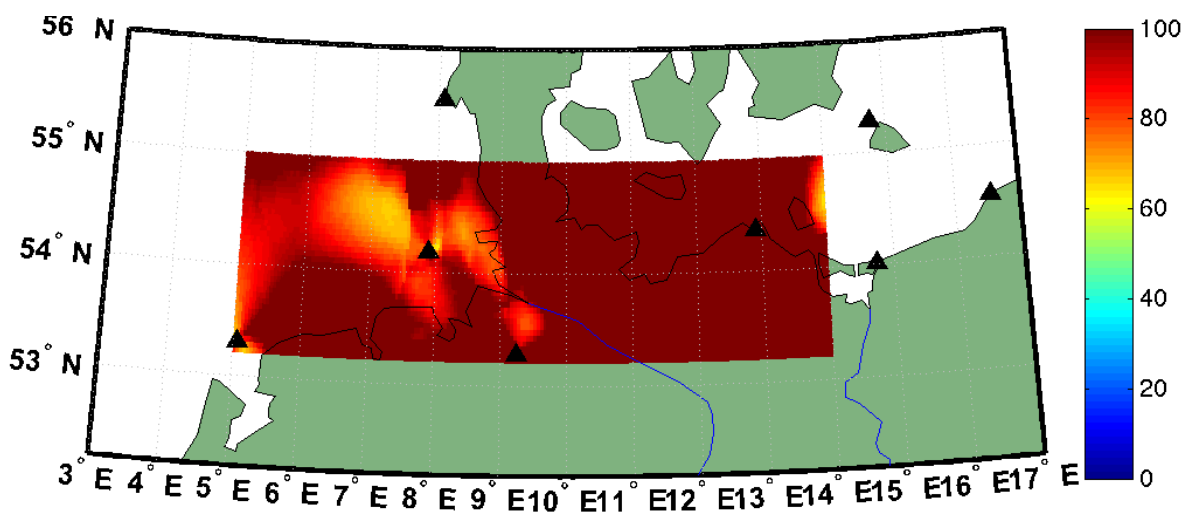


Figure 30: Lower bound to positioning accuracy of MF DGNSS R-Mode on region II – night.

The combined bounds on performance are shown in Figure 31 (day) and Figure 32 (night). Adding AIS improves the performance during the day only slightly since the MF DGNSS performance during the day is already quite good. The prime advantage would be as an additional aid to the ambiguity resolution (as opposed to beat frequencies or the defined RTCM message). At night, the MF DGNSS performance alone is worse, and the AIS is good only near the AIS stations; combining the two increases the area of good performance somewhat over AIS alone.



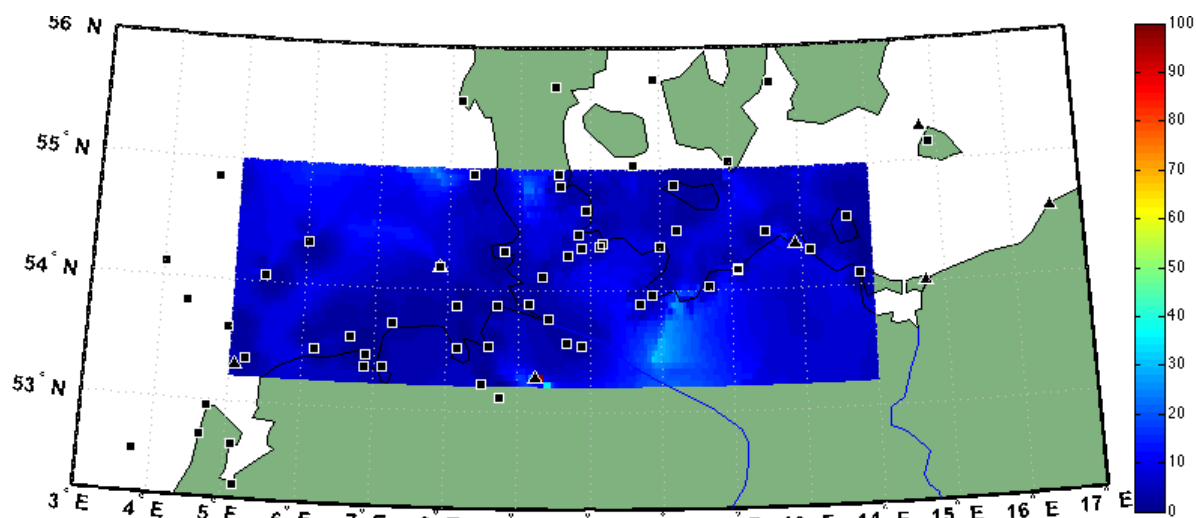


Figure 31: Lower bound to positioning accuracy of combined MF DGNSS and AIS R- Mode on region II– day. MF beacon locations are triangles, AIS stations are squares.

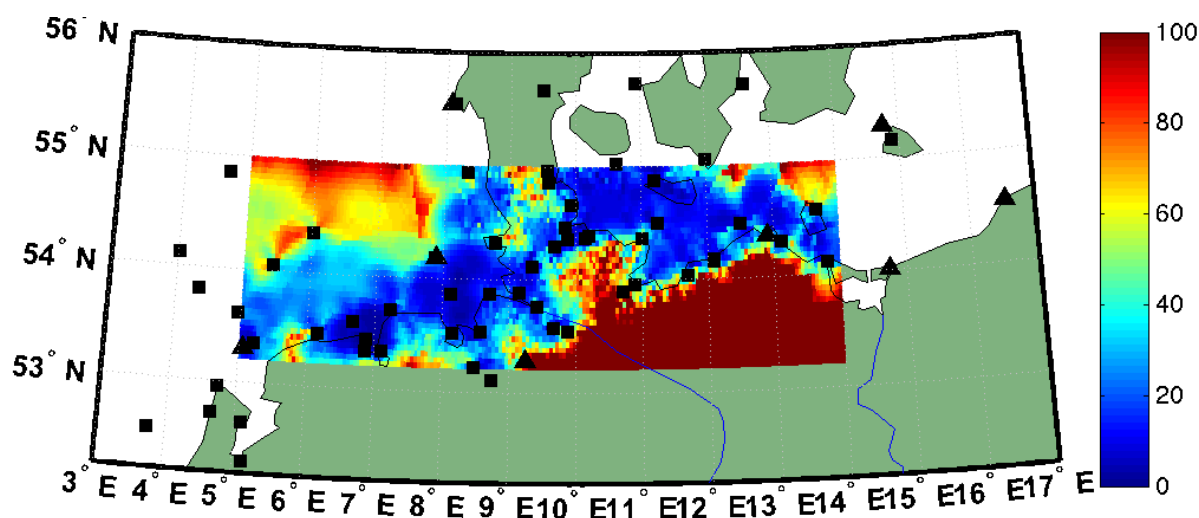


Figure 32: Lower bound to positioning accuracy of combined MF DGNSS and AIS R- Mode on region II– night. MF DGNSS beacon locations are triangles, AIS stations are squares.

We note the following:

- During the day, the only real benefit to the combination is AIS can be used to aid in the ambiguity resolution on the MF DGNSS.
- At night, combining MF DGNSS and AIS provides slight improvement over AIS alone.
- Although there is a high density of both MF DGNSS and AIS stations in the North Sea area, this is not globally true; so combining AIS and MF DGNSS could make positioning possible in areas where there is insufficient of either type of station alone.

### 3.4 MF DGNSS, AIS, and eLoran

#### 3.4.1 Region II

Continuing to focus on region II, we now consider the addition of eLoran to MF DGNSS and AIS. Due to the uncertainties with the future of eLoran we present only the improvements possible by including a single Loran tower (Sylt in Figure 33) or using two (Sylt and Anthorn in Figure 35).

We note the following:

- Adding even a single Loran station improves performance over that of MF DGNSS and AIS alone.
- Adding two Loran stations improves performance over using just one.

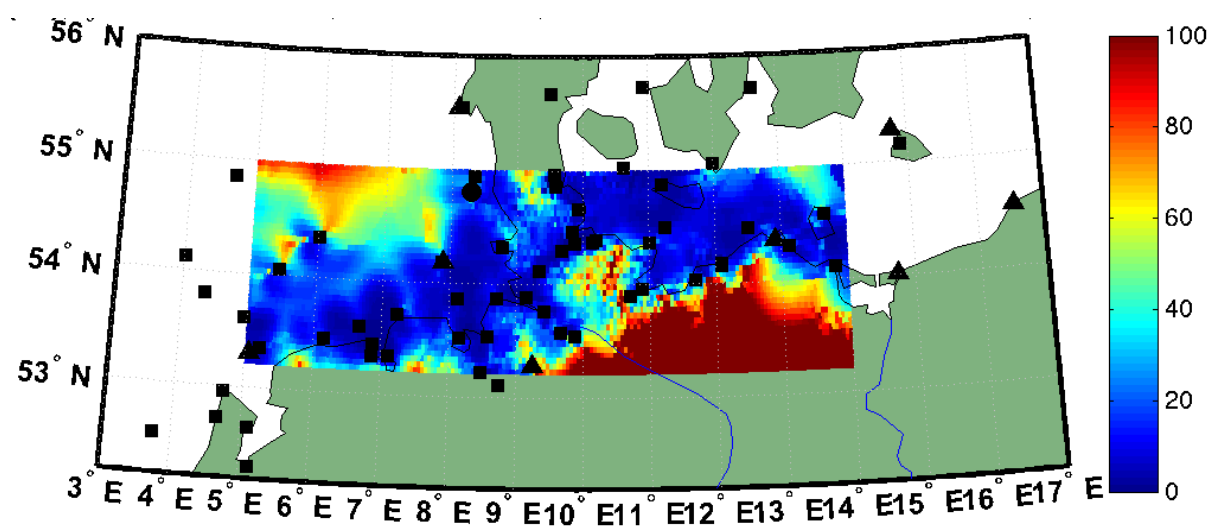


Figure 33: Lower bound to positioning accuracy of combined MF DGNSS-AIS-eLoran (Sylt only) on region II- night.

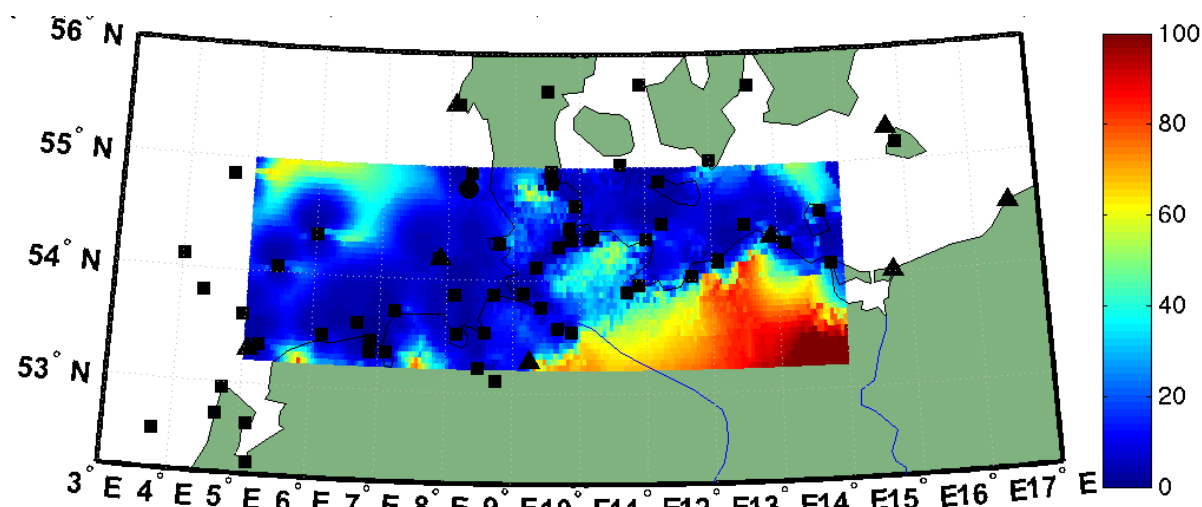
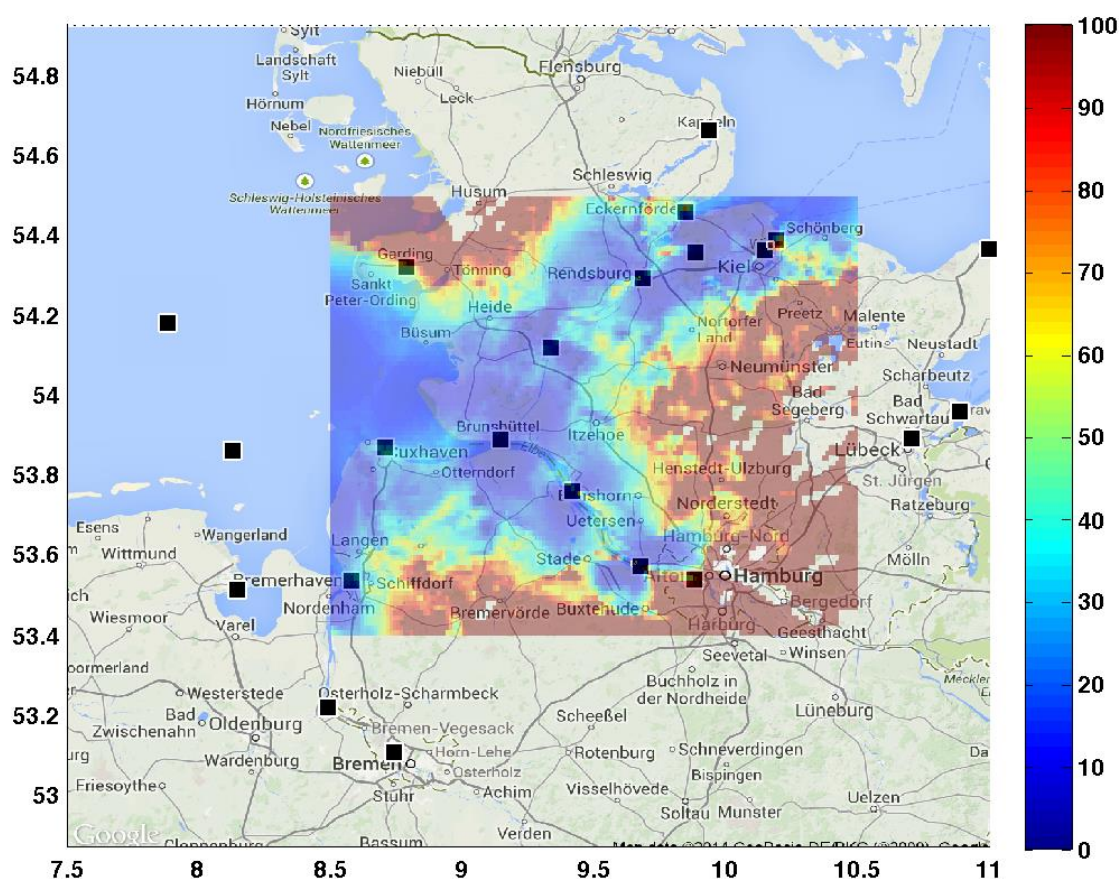


Figure 34: Lower bound to positioning accuracy of combined MF DGNSS-AIS-eLoran (Sylt and Anthorn) on region II- night.

### 3.4.2 Region III

The Milestone 4 report [6] also recognized that some portions of this study area are more important than others; for example, the waterways of the Kiel Canal and the Elbe River as far as Hamburg. A secondary analysis focused on these waterways inside a boundary box of  $8.5^{\circ} - 10.5^{\circ}$  E longitude and  $53.4^{\circ} - 54.5^{\circ}$  N latitude (region III). Figure 35 shows the potential performance in this region for AIS R-Mode alone. While some portions of this area appear to have performance better than 10-20 m, the performance on the canal and river, themselves, is limited (some areas of 60-70m performance) by the fact that the existing AIS transmitters follow the waterways, effectively in a straight line (which is poor from a DOP perspective). In [6] we demonstrated that it would be possible to improve AIS R-Mode performance along the canal and river by including the AIS base station at Hamburg (operated by the Port of Hamburg) and adding several new AIS transmitter sites.



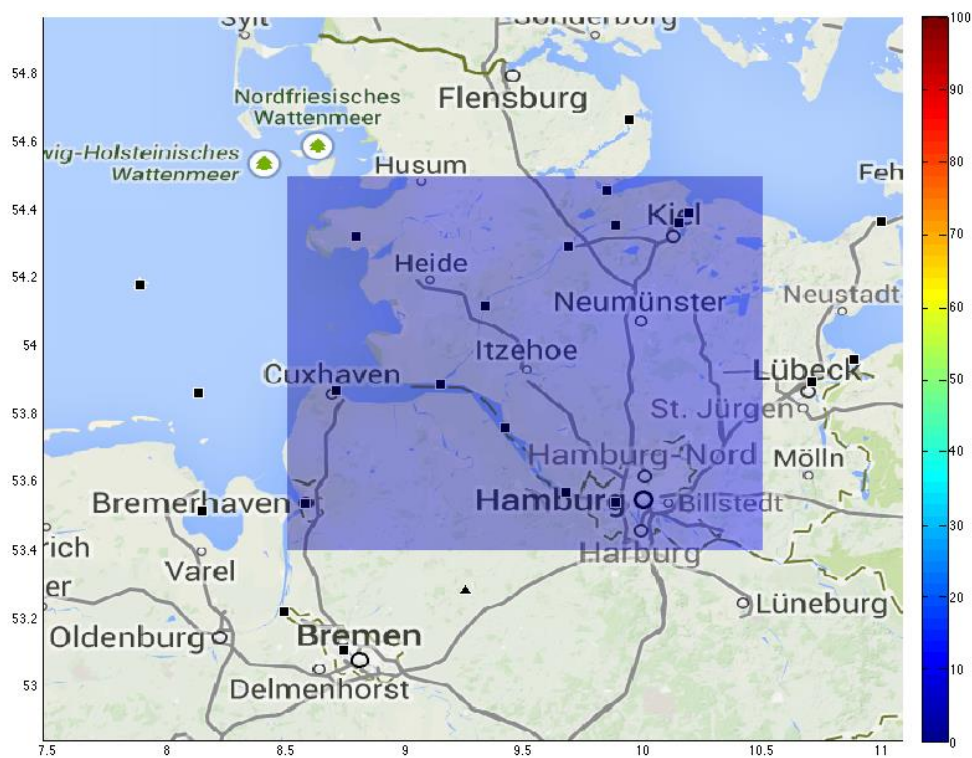
**Figure 35: Lower bound to positioning accuracy of AIS R-Mode on region III (in meters). AIS sites are squares.**

Another option to improve performance along these critical waterways would be to combine existing MF DGNSS, AIS, and/or eLoran signals in this area. Several combinations are possible. In the figures that follow, AIS sites are squares, MF DGNSS sites are triangles, and eLoran sites are circles.

**As a first option consider combined AIS and MF DGNSS R-Mode.** Note that the performance is uniformly better than 10 meters (blue shading) throughout the region.

Figure 36 shows the resulting performance bound for day; not unexpectedly (based upon Figure 10), the performance is excellent. Figure 37 shows the performance bound for night; even though MF DGNSS R-Mode is susceptible to sky wave, we do see small improvement near Hamburg.





Note that the performance is uniformly better than 10 meters (blue shading) throughout the region.

**Figure 36: Combined AIS and MF GNSS R-Mode performance on region III – day; AIS sites are squares, MF DGNSS sites are triangles.**

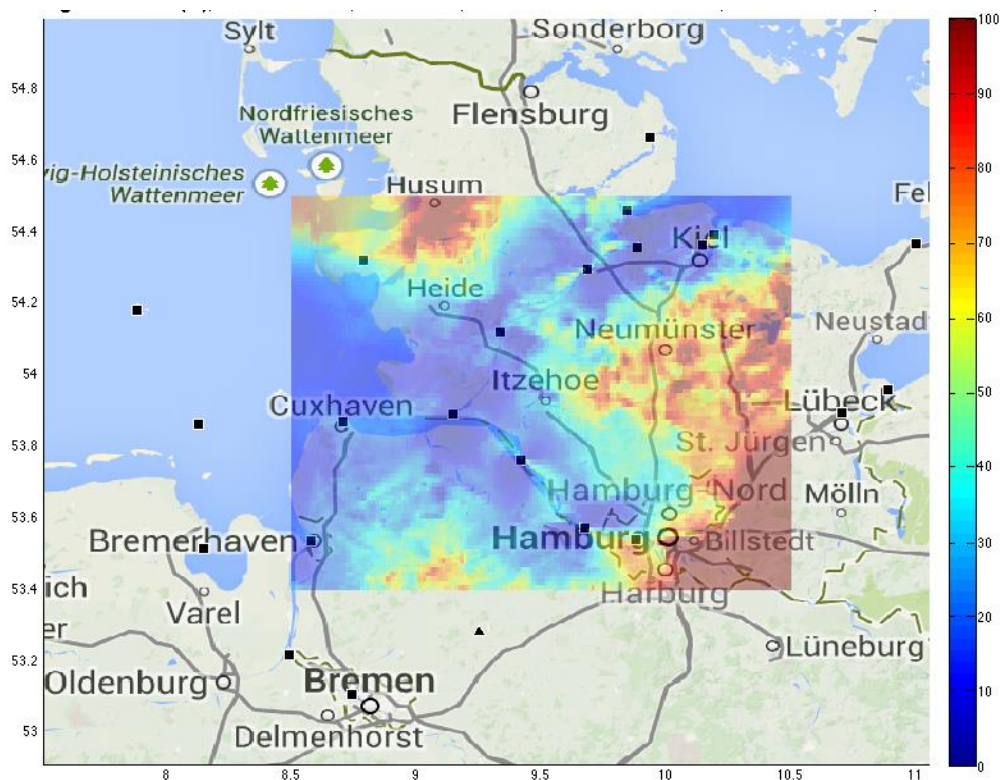


**Figure 37: Combined AIS and MF DGNSS R-Mode performance on region III – night. AIS sites are squares, MF DGNSS sites are triangles.**

A second option would be to combine AIS and eLoran. Since the AIS performance along the canal and river are primarily limited by geometry, consider the addition of only the Loran signal from Sylt. Figure 38 shows the resulting performance bound. In comparison to Figure 35 performance along the canal and river are much improved.

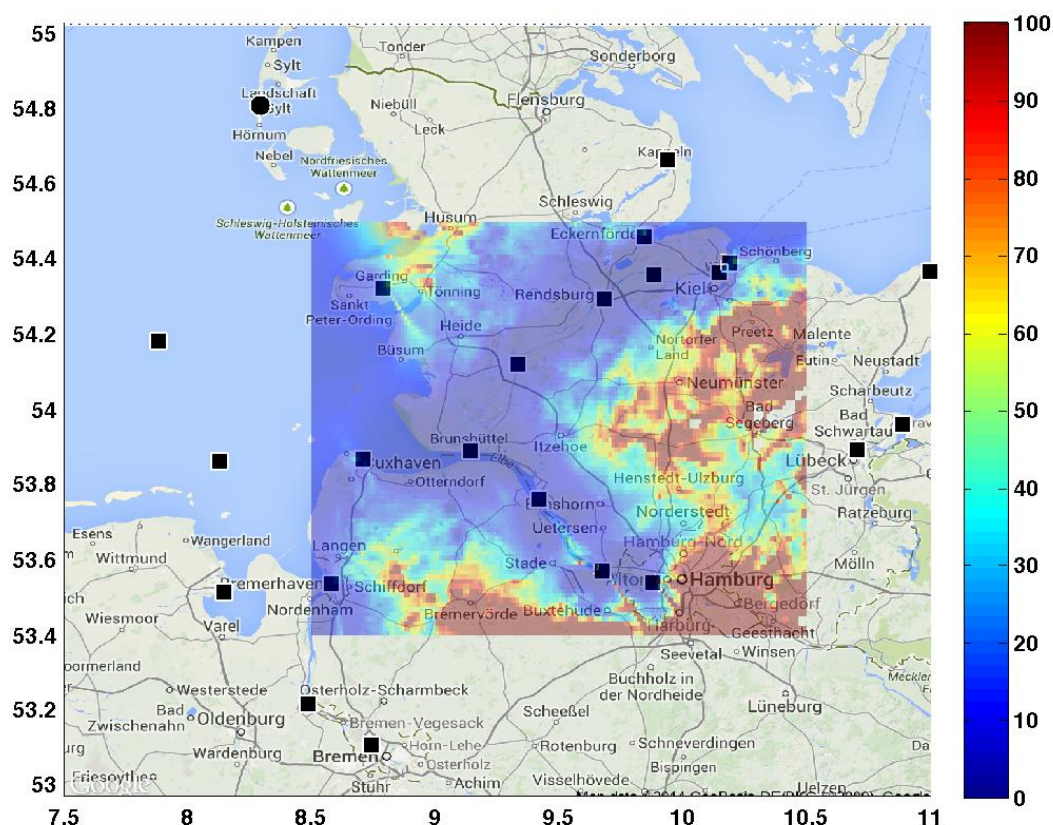


**Figure 38: Lower bound to positioning accuracy of combined AIS and eLoran (Sylt only) on region III. AIS sites are squares, Sylt is a circle.**

Finally, consider combining AIS, MF DGNSS, and eLoran. Figure 39 shows the resulting night performance bound (Sylt only). As expected there is slight improvement, but not especially along either critical waterway. Including Anthorn as well (Figure 40), improves performance some as expected.



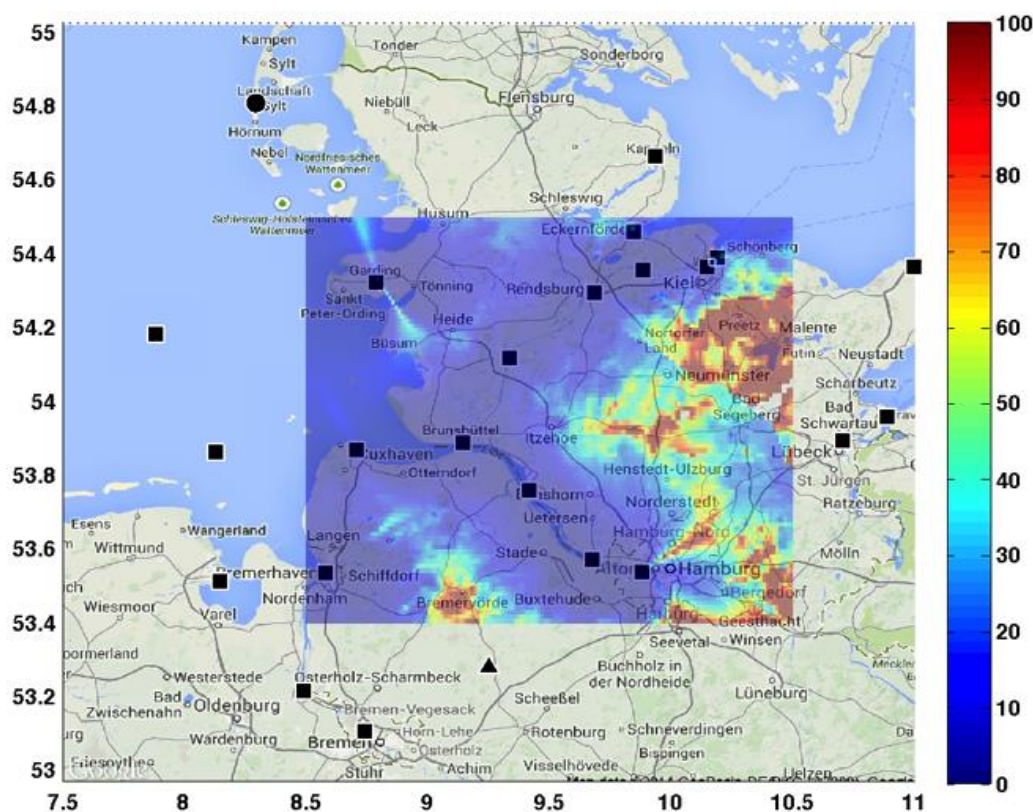


**Figure 39: Combined MF DGNSS, AIS, and eLoran (Sylt only) on region III – night. AIS sites are squares, MF DGNSS sites are triangles, Sylt is a circle.**

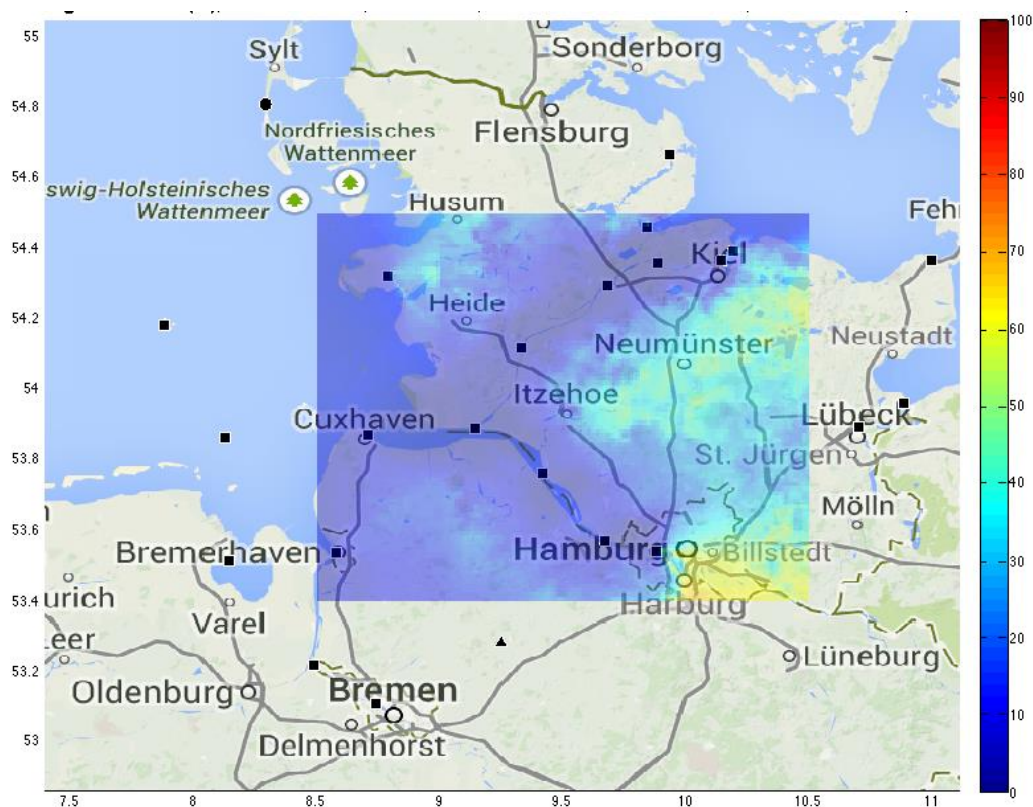


**Figure 40: Combined MF DGNSS, AIS, and eLoran (Sylt and Anthorn) on region III – night. AIS sites are squares, MF DGNSS sites are triangles, Loran are circles.**



We note the following for the various options in region III:

- Focused on night as limiting case (for MF DGNSS).
- During the night, no individual system provides 100% high-accuracy coverage along the critical waterways.
- During the night, the combination of eLoran and AIS provides good high-accuracy coverage (slightly better than AIS-MF DGNSS).
- Adding MF DGNSS to AIS and eLoran improves performance over AIS and eLoran alone.

### 3.5 Test Bed Design

There are two options for implementing a combined R-Mode test bed: 1) locate it near the test transmitter in IJmuiden, or 2) install a test modulator at another location. We have identified three potential test beds, covering both options, and give options for a domestic (German-only) test bed or one in partnership with other countries (Denmark or Netherlands).



**Figure 41: IJmuiden test transmitter with 100km range ring; AIS sites are red dots, MF DGNSS test transmitter is black dot.**

#### 3.5.1 Test Bed Option 1 – German-Dutch

Since the MF DGNSS test modulator is being installed at IJmuiden, it makes sense to consider this area as a potential multi-system R-Mode test bed. Figure 41 shows the location of the MF DGNSS transmitter at IJmuiden (black dot) along with the predicted 100km range (black circle). The nearby AIS stations are all shown as red dots. In order to keep to a constrained test bed area, a small area near IJmuiden is proposed. This area (see Figure 42) uses the IJmuiden MF DGNSS transmitter (triangle), 6 nearby AIS transmitters (squares), and the Sylt eLoran tower (circle) and covers the area of the Markermeer and IJsselmeer areas North of Amsterdam as well as the Noordzee Kanaal (North Sea canal) and its approaches. Figure 42 shows the predicted position performance for the proposed test bed area. Day performance is shown; performance at night is similar. Although the predicted

performance is not shown south of 52.2°N latitude, IJmuiden would offer coverage of Rotterdam as well, so testing could also be conducted in that area if desired, by using AIS stations around Rotterdam.

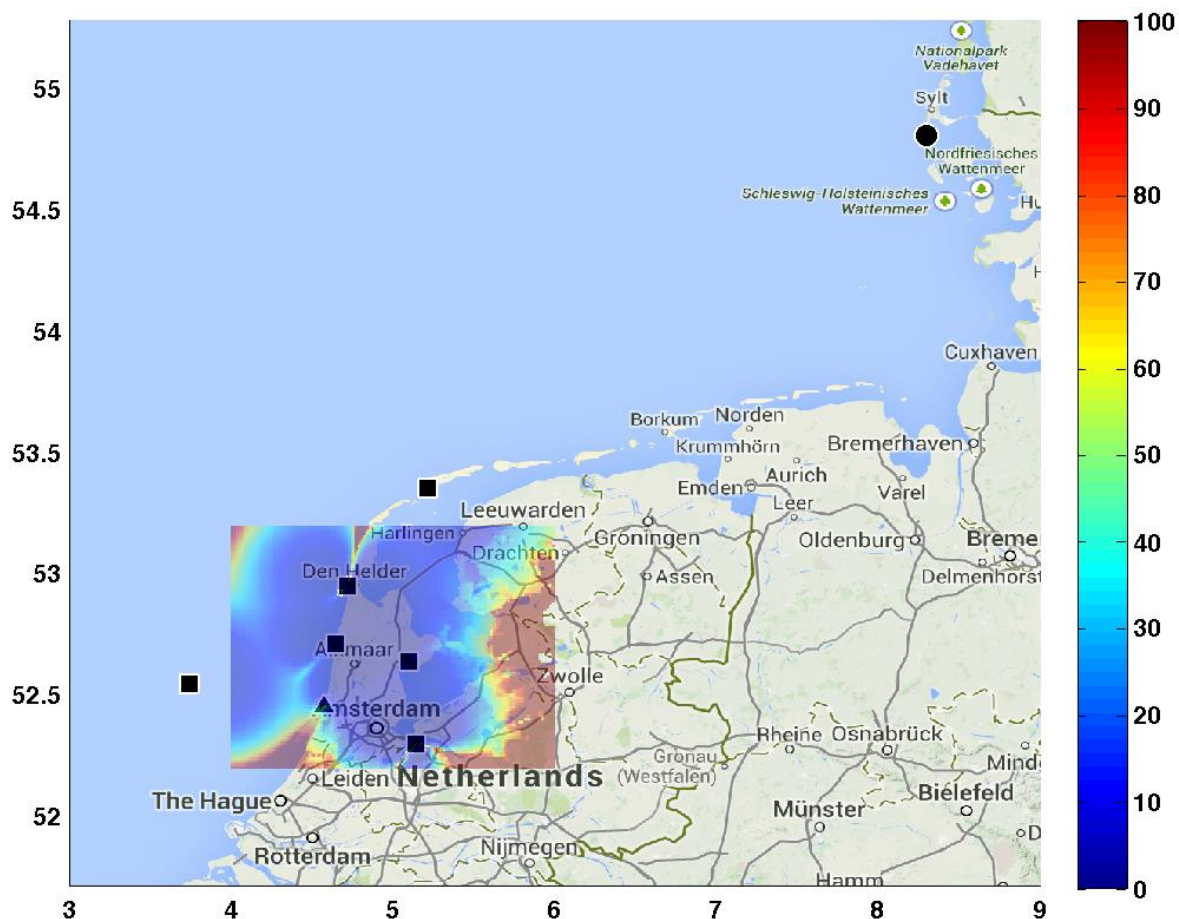


**Figure 42: Option 1 for a test bed area near IJmuiden. Predicted coverage accuracy using AIS, MF DGNSS, and eLoran (Sylt only) R-Mode during the day (night coverage is similar).**

### 3.5.2 Test Bed Option 2 – German

This test bed is region III (as described previously). Figure 43 shows the location of the MF DGNSS transmitter at Zeven (triangle, just south of the region), the nearby AIS stations (squares), and eLoran station Sylt (circle, northwest of the region) along with the predicted position performance for the proposed test bed area. Day performance is shown; performance at night is similar. This test bed would allow assessment on the Kiel Canal and Elbe River and their approaches.

This test bed is a larger area than option 1, and covers the critical waterways of the Kiel Canal and Elbe River. For this option a MF DGNSS test transmitter would need to be installed at Zeven (this could be a new one or the one from IJmuiden relocated). There are numerous AIS transmitters in the area that could be used. The test could also be focused on just part of the area if desired, and fewer AIS transmitters used.

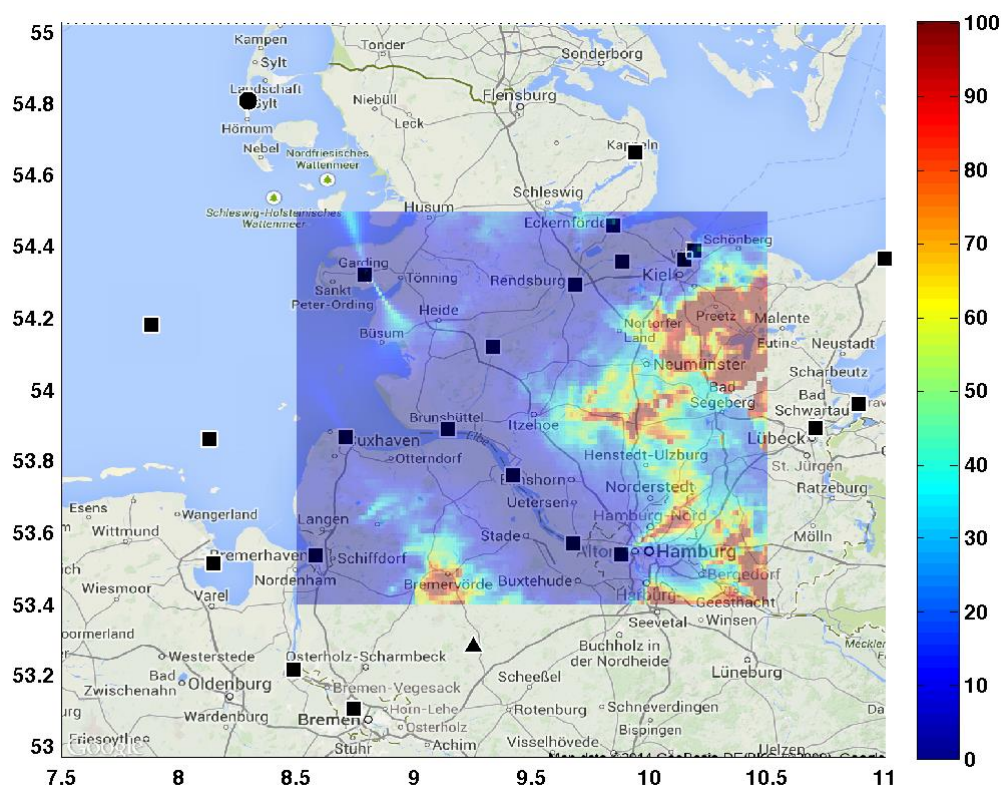


**Figure 43: Option 2 for a test bed area near the Kiel Canal and Elbe River.**  
**Predicted coverage accuracy using AIS, MF DGNSS, and eLoran (Sylt only) R-Mode during the day (night coverage is similar).**

### 3.5.3 Test Bed Option 3 – German-Danish

This western Baltic Sea test bed is the area proposed as the joint German-Danish AIS test bed in the Milestone 4 report [6]. Figure 44 shows the predicted position performance for the proposed test bed area during the night; the daytime performance would be slightly better. The same 5 AIS transmitters used in [6] are used again. The only close MF DGNSS site is Groß Mohrdorf (located about 115km to the east). Only a single Loran station (Sylt) was included; adding in Anthorn does not change the picture appreciably. Sylt is located about 115 km to the west.

This test bed is similar size to that in option 1, and covers the eastern approaches to the Kiel Canal. For this option a MF DGNSS test transmitter would need to be installed at Groß Mohrdorf (this could be a new one or the one from IJmuiden relocated). This test bed has the advantage of a ferry route running through the middle of the test area; the ferry could be a convenient data collection platform.



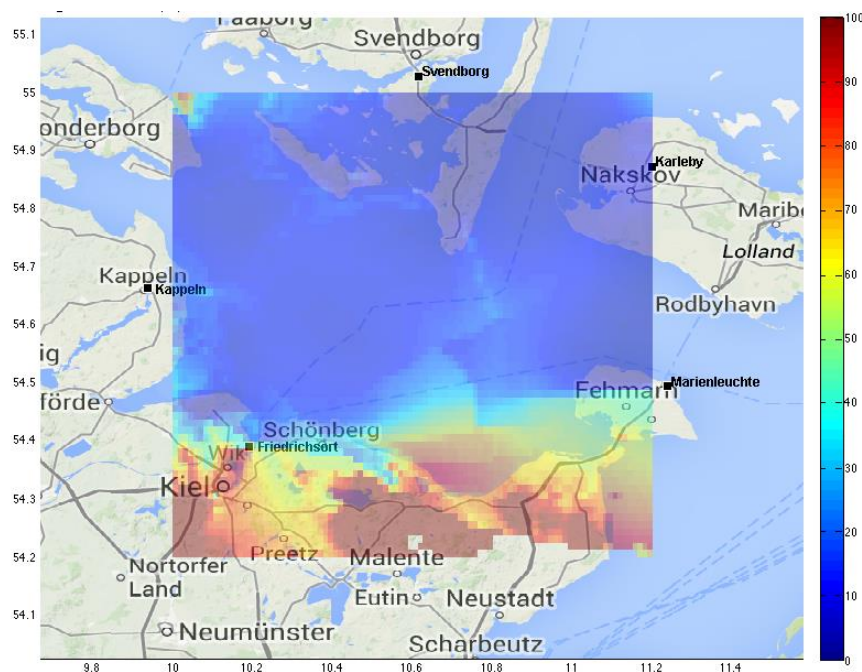


**Figure 44: Option 3 for a joint German-Dutch test bed area. Predicted coverage accuracy using AIS (squares), MF DGNSS (Groß Mohrdorf to East, not visible), and eLoran (Sylt only, not visible on map) R-Mode during the night.**

## 4 Conclusions

There are currently no existing standards established for the required position or time accuracy for a backup PNT system. We have considered performance at the 10m or better level to be excellent; however, for a backup system, 100m may be entirely sufficient. Keeping this in mind, we repeat the following assertions from the previous Milestone reports ([3, 6]):

- **MF DGNSS R-Mode is a backup to GNSS that can meet the resilient PNT requirements of e-Navigation.** The predicted daytime bound on R-Mode positioning using TOA accuracy bounds is very good – better than 10m accuracy in most of the North Sea Area. Using our pessimistic sky wave assumptions, the R-Mode performance at night is about a factor of 10 worse than daytime performance, but still better than 100m accuracy for most of the North Sea Area.
- **AIS R-Mode is a backup to GNSS that can meet the resilient PNT requirements of e-Navigation.** Predicted accuracy of 10m appears achievable using the existing system with **no** modifications other than adding some additional transmissions. There is also no day / night difference in system performance.

While both display the potential for SoOP positioning, the MF DGNSS and AIS signals have some limitations in an R-Mode application:

- MF DGNSS ranging (based upon the CW carrier phase) appears to offer good performance during the day, but its performance is limited by sky wave interference at night. Further, the carrier cycle ambiguity must be resolved so as to yield a unique position solution.
- AIS ranging (based on the bit edge) is not impacted by sky wave (being a line of sight signal), but has limited coverage due to the finite range of this LOS propagation.

Conceptually, combining the signals together in an “all-in-view” R-Mode receiver, and potentially including eLoran in the mix (which is currently available in the North Sea area), should yield improved positioning performance. Several combinations were considered on different areas in and around the North Sea.

The combination of MF DGNSS and eLoran was explored in an area (region I) covering a large part of the North Sea. Similar to the MF DGNSS and AIS combination, performance pretty much matched that of the better individual system. In other words, the existing eLoran network provides good performance in region I as does the MF solution during the day. In the event that there was not a full eLoran network, adding even just a single eLoran station (such as Sylt) can improve the performance of the MF DGNSS solution at night. In addition, any such signal can help with the required MF cycle ambiguity resolution. Finally, even a single strategically positioned eLoran station can provide cost-efficient time transfer for all R-Mode MF and AIS shore stations in the area; precise timing of transmissions is one of the fundamental pre-requisites for any R-Mode at MF and/or AIS shore stations in the region.

The combination of MF, AIS, and eLoran was explored in an area (region II) containing the German bight and parts of the western Baltic Sea. During the day, MF DGNSS ranging alone appeared to offer good performance due to the high density of MF beacons in the region; the only real benefit of the combination with AIS is that the AIS bit edge can be used to aid in ambiguity resolution on the MF CW signal. At night, the combination of MF DGNSS and AIS R-Mode showed some improvement over AIS R-Mode alone. We note, however, there is a high density of both MF DGNSS and AIS (base station) transmitters in the region examined. This is not globally true (e.g. the density of MF DGNSS beacons in the United States is low), so combining AIS and MF DGNSS signals could make positioning possible in areas where there is insufficient of either type of signal alone. In addition, it is clear that including even a single Loran signal in the mix, improves performance.

The combination of MF, AIS, and eLoran was explored in a small area around the Kiel Canal (region III). In this area all three signals themselves are limited: MF is limited by fewer signals and sky wave at night; AIS base stations, while plentiful, have poor geometry and limited range; and the region is outside of the eLoran triads so exhibits poor eLoran DOP. Combining signals, it was seen that good positioning performance can be achieved, even during the night. As expected, the more signals, the better the performance.

Table 2 summarizes the potential synergy gained by combining signals. The table separates MF DGNSS into both day and night entries due to the significant difference in potential performance. Similarly, eLoran is separated depending upon the number of transmitters operating (all 5 visible in the North Sea or just Sylt). The performance has been “graded” on a 4-point scale where

- 1 = 0 – 10m position accuracy over most of the area
- 2 = 0 – 20m position accuracy over most of the area
- 3 = 0 – 50m position accuracy over most of the area
- 4 = 0 – 100m position accuracy over most of the area

This assessment is somewhat subjective in regards to the “most of the area” part, but is sufficient to enable relative comparisons between the various options. As expected, the best performance can be achieved using ALL signals. Performance at night is slightly worse than during the day due to the reduced MF DGNSS performance at night. For example, MF DGNSS-AIS renders a 1 during the day and a 3 at night, which is better than a 4 at night for MF DGNSS alone or a 3 for AIS alone (day or night). A single Loran station can provide a large improvement at night over a large coverage area. For example, Sylt alone can cover the North and Baltic Seas sufficiently as an R-Mode signal to supplement AIS or MF DGNSS R-Mode; it is a very efficient augmentation to AIS R-Mode.

**Table 2: Pairwise synergy of the signal choices.**

1 = 0-10m, 2 = 0-20m, 3 = 0-50m, and 4 = 0-100m position accuracy over most of the area

System	Performance
MF DGNSS(day)-AIS-eLoran(1)	1
MF DGNSS(day)-AIS	1
MF DGNSS(day)-eLoran(1)	2
MF DGNSS(night)-AIS-eLoran(1)	2
AIS-eLoran(1)	2
MF DGNSS(day)	2
MF DGNSS(night)-AIS	3
AIS	3
eLoran (5)	3
MF DGNSS(night)-eLoran(1)	4
MF DGNSS(night)	4
eLoran (1)	n/a

In summary, depending upon availability, 1 or 2 eLoran signals can be combined with AIS and MF DGNSS to offer improved performance. In general, performance results are strongly position dependent – in many areas one system (signal type) dominates performance. Also, as expected, more signals results in increased performance (or at least no worse). **To achieve widespread resilient PNT, the best solution is to use all signals available in a true all-in-view receiver.**

It should be noted that the coverage analysis has been based on using existing sites only. Additional sites could certainly be added (eLoran, MF DGNSS, or AIS) in areas where needed. A cost-benefit analysis to address the benefits of adding sites has not been part of this feasibility study and would need to be done on an area-by-area basis. This is left as work for the future. In addition, the position and time requirements for a back-up system have **not** been internationally established yet; this would need to be done prior to undertaking a cost-benefit analysis.

Finally, it is important to note that the need for a backup PNT is not uniform. The performance of a backup PNT system is most critical in the areas with the highest density of shipping traffic. Referring back to Figure 5, it is clear that ship traffic is concentrated in certain areas. These areas also have the largest number of AIS and MF DGNSS transmitters nearby and thus the R-Mode performance is best in these areas. Figure 46 shows the predicted R-Mode performance for region II overlaid on top of the ACCSEAS shipping density plot to illustrate this alignment; the areas of highest density traffic (dark black tracks) are almost entirely in the areas with the best predicted performance (dark blue shading). Figure 46 is the same figure but with the predicted R-Mode performance shaded according to the four performance levels used in Table 2. It is likely that this alignment of R-Mode performance with the high density shipping lanes will be true in other parts of the world as well, since those are the areas with the largest numbers of AIS (and MF DGNSS) stations.



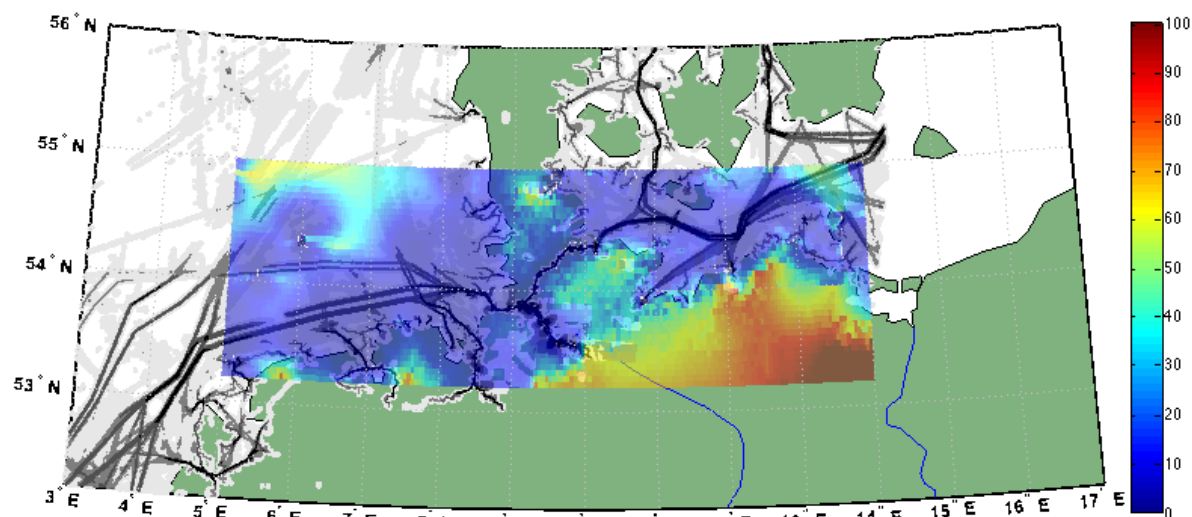


**Figure 45: R-Mode performance overlaid on top of shipping density plot.**  
Predicted R-Mode performance shaded using 0-100m accuracy scale. Shipping density shaded so that darker is higher density traffic.

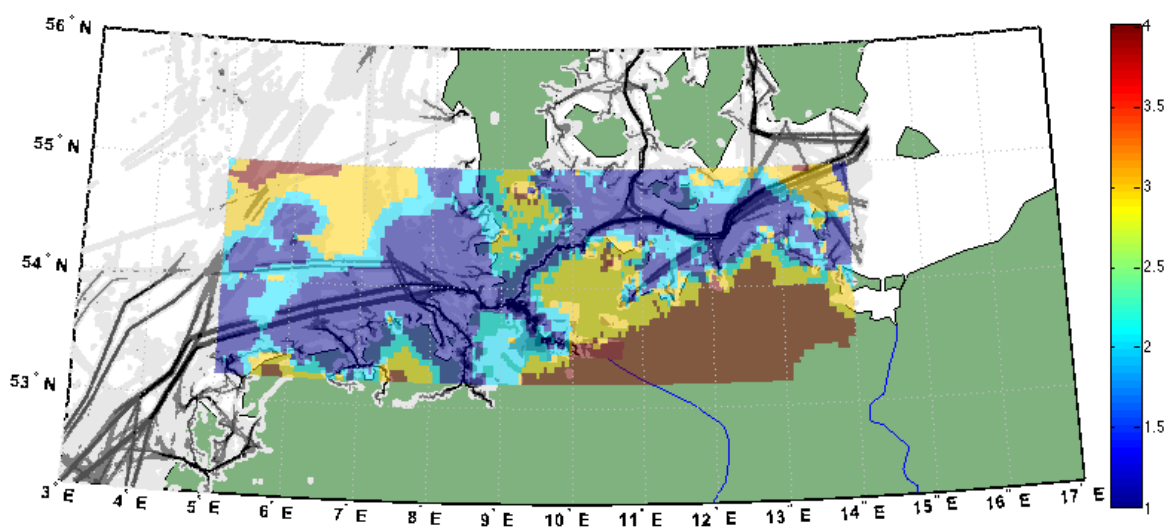


**Figure 46: R-Mode performance overlaid on top of shipping density plot.**  
Predicted R-Mode performance shaded using 4-point scale defined for Table 2. Shipping density shaded so that darker is higher density traffic.

Three test beds were proposed for further assessment of combined R-Mode positioning: one on the Dutch coast exploiting the new IJmuiden MF transmitter, one near the Kiel Canal and Elbe River (region III), and one in the western Baltic Sea. Establishing a test bed would allow for assessing the performance of a real-world receiver (versus the predicted lower bounds on performance) and also to investigate the impact of time synchronization and propagation effects.

## 5 References

- [1] T. Porathe, "ACCSEAS Baseline and Priorities Report," 2013.
- [2] "The e-Navigation Architecture - the Shore-based Perspective, 2nd Edition DRAFT," International Association of Marine Aids to Navigation and Lighthouse Authorities (IALA), Saint Germain en Laye, France, IALA Recommendation e-NAV-140, December 2013.
- [3] G. W. Johnson and P. F. Swaszek, "Feasibility Study of R-Mode using MF DGPS Transmissions," German Federal Waterways and Shipping Administration, Milestone 2 Report, 11 March 2014.
- [4] G. W. Johnson, P. F. Swaszek, R. Hartnett, R. Shalaev, C. Oates, D. Lown, *et al.*, "A Procedure for Creating Optimal ASF Grids for Harbor Entrance & Approach," presented at the ION GNSS 2006, Fort Worth, TX, 2006.
- [5] P. Williams and D. Last, "Mapping the ASFs of the Northwest European Loran-C System," in *28th Annual Convention and Technical Symposium, International Loran Association*, 1999.
- [6] G. W. Johnson and P. F. Swaszek, "Feasibility Study of R-Mode using AIS Transmissions," German Federal Waterways and Shipping Administration, Milestone 4 Report, 25 July 2014.
- [7] G. Johnson, P. Swaszek, L. Hartshorn, R. Hartnett, and M. Wiggins, "Possible Optimizations for the US Loran System," presented at the IEEE/ION PLANS 2006, San Diego, CA, 2006.
- [8] P. Williams, C. Hargreaves, D. Last, and N. Ward, "eLoran in the UK: Leading the Way," presented at the ION 2013 Pacific PNT Meeting, Honolulu, HI, 2013.
- [9] R. Hartnett, K. Gross, G. Czerwonka, H. Holland, M. Narins, C. Oates, *et al.*, "Digital Down Converter (DDC) H-Field Loran-C Navigation Receiver: Performance Analysis, Flight Test Update, and GPS/WAAS Integration," in *Institute of Navigation National Technical Meeting*, San Diego, CA, 2002.
- [10] G. L. Roth, P. Schick, C. A. Schweitzer, J. Jacoby, D. J. Gervasi, and R. Ferrier, "New eLoran Receiver and Antenna Technology for Integrated GPS/Loran Systems," in *Institute of Navigation, National Technical Meeting*, San Diego, CA, 2005.
- [11] A. W. Helwig, G. W. Offermans, C. Schue, B. Walker, T. Hardy, and K. Zwicker, "Low Frequency (LF) Solutions for Alternative Positioning, Navigation, Timing, and Data (APNT&D) and Associated Receiver Technology," RTCM Paper 058-2011-SC123-088, 2011.
- [12] K. Montgomery, "Enhanced LORAN Receiver (ELR)," in *International Loran Association Symposium*, Orlando, FL, 2007.
- [13] Z. Conover, "Integrated eLoran/GPS Receiver Development Platform," in *International Loran Association Symposium*, Orlando, FL, 2007.
- [14] A. W. Helwig, G. W. Offermans, R. Kellenbach, W. J. Pelgrum, and D. van Willigen, "Pushing the Performance Limits of Loran-C/Eurofix Receivers," in *Proceedings of the 3rd International Symposium on Integration of Loran-C / Eurofix and EGNOS / Galileo*, Munich, Germany, 2002.
- [15] B. Peterson, "Electronic Navigation Systems," in *The Electronics Handbook*. vol. Chapter 113, J. Whitaker, Ed., ed Boca Raton, FL: CRC Press, 1996, pp. 1710-1733.
- [16] R. Yarlagadda, I. Ali, N. Al-Dhahir, and J. Hershey, "GPS GDOP metric," *Radar, Sonar and Navigation, IEE Proceedings -*, vol. 147, pp. 259-264, 2000.